

Preliminary Mariner 9 Report on the Geology of Mars¹

J. F. McCUALEY², M. H. CARR², J. A. CUTTS³, W. K. HARTMANN⁴,
HAROLD MASURSKY², D. J. MILTON², R. P. SHARP⁵, AND D. E. WILHELM²

Received June 7, 1972

Mariner 9 pictures indicate that the surface of Mars has been shaped by impact, volcanic, tectonic, erosional and depositional activity. The moonlike cratered terrain, identified as the dominant surface unit from the Mariner 6 and 7 flyby data, has proven to be less typical of Mars than previously believed, although extensive in the mid- and high-latitude regions of the southern hemisphere. Martian craters are highly modified but their size-frequency distribution and morphology suggest that most were formed by impact. Circular basins encompassed by rugged terrain and filled with smooth plains material are recognized. These structures, like the craters, are more modified than corresponding features on the Moon and they exercise a less dominant influence on the regional geology. Smooth plains with few visible craters fill the large basins and the floors of larger craters; they also occupy large parts of the northern hemisphere where the plains lap against higher landforms. The middle northern latitudes of Mars from 90 to 150° longitude contain at least four large shield volcanoes each of which is about twice as massive as the largest on Earth. Steep-sided domes with summit craters and large, fresh-appearing volcanic craters with smooth rims are also present in this region. Multiple flow structures, ridges with lobate flanks, chain craters, and sinuous rilles occur in all regions, suggesting widespread volcanism. Evidence for tectonic activity postdating formation of the cratered terrain and some of the plains units is abundant in the equatorial area from 0 to 120° longitude. Some regions exhibit a complex semiradial array of graben that suggest doming and stretching of the surface. Others contain intensely faulted terrain with broader, deeper graben separated by a complex mosaic of flat-topped blocks. An east-west-trending canyon system about 100–200 km wide and about 2500 km long extends through the Coprates-Eos region. The canyons have gullied walls indicative of extensive headward erosion since their initial formation. Regionally depressed areas called chaotic terrain consist of intricately broken and jumbled blocks and appear to result from breaking up and slumping of older geologic units. Compressional features have not been identified in any of the pictures analyzed to date. Plume-like light and dark surface markings can be explained by eolian transport. Mariner 9 has thus revealed that Mars is a complex planet with its own distinctive geologic history and that it is less primitive than the Moon.

INTRODUCTION

Mars, as revealed to Mariner 9 after the great dust storm of 1971, proved to be

¹ Publication authorized by the Director, U.S. Geological Survey.

² U.S. Geological Survey, Flagstaff, AZ, and Menlo Park, CA.

³ Jet Propulsion Laboratory, Pasadena, CA.

⁴ Science Applications, Inc., Tucson, AZ.

⁵ California Institute of Technology, Pasadena, CA.

geologically far more heterogeneous than previously suspected (Masursky *et al.*, 1971). Certain regions of the planet have been shaped principally by impact, others by volcanism. Tectonism, erosion, and deposition appear to dominate other parts of the surface. The dominant geological processes that have shaped the surface of Mars have varied not only from place to place but also from time to time throughout the planet's history.

The equatorial region displays most of the distinctive geologic features of Mars although some features appear to be restricted to the high-latitude and polar regions described in a companion paper (Murray *et al.*, 1972). This region (30° south latitude to 30° north latitude), an area of about $8 \times 10^7 \text{ km}^2$ or roughly 10 times the area of the conterminous United States of America, is depicted in four geologic sketch maps. The rationale and methods employed in the mapping were similar to those used for the Moon as described by Wilhelms and McCauley (1971) and McCauley and Wilhelms (1971). The maps, along with brief descriptions of the geological units portrayed, are followed by a series of more interpretative discussions dealing with topical problems and a summary geologic history.

UNIT DESCRIPTIONS

Seventeen geologic units are defined and mapped on the basis of their textural characteristics (Figs. 1–5). A-frame pictures of the reference or type area for each unit are given in succeeding figures.

Materials associated with craters 100 km in diameter and larger were divided into three units. A progression in crater sharpness similar to that described for the Moon by Pohn and Offield (1971) is apparent. The two main crater units are distinguished on the basis of morphologic sharpness. Younger craters (c_2) are characterized principally by the preservation of a surrounding ejecta blanket (Fig. 6). Older craters (c_1) are severely degraded, lack recognizable ejecta blankets, and are generally shallower than c_2 craters. Even the freshest craters mapped are far more degraded than lunar craters of equivalent size. No crater resembling Tycho or Copernicus has been identified on Mars. Five large, elliptical troughs surrounded by rough, raised rim deposits have been distinguished as irregular craters (ci). These are grossly similar in form to the lunar crater Schiller (Fig. 7). In contrast to the circular craters which are considered to be of impact origin, these irregular features are difficult to explain other than by internal

processes, that is, by some combination of tectonic and volcanic activity.

Areas dominated by craters not exceeding 100 km in diameter have been mapped as cratered terrain (dc or mc). Within the densely cratered terrain, craters are closely spaced or contiguous and most are severely degraded; the intercrater areas are rougher than for unit mc. Within the moderately cratered terrain, craters are more widely spaced and the intercrater areas are undulating and are not distinctive (Fig. 8). The cratered plains unit (cp) is characterized by scattered, moderately sharp-appearing craters mostly smaller than 100 km in diameter (Fig. 9). Complex linear ridges, many of which have lobate flanks, are common. This unit tends to be darker than surrounding units and grossly resembles the lunar maria. The unit is more extensive than shown on the map and lies in many small patches throughout the equatorial region—only the largest and most continuous occurrences are shown.

Three types of volcanic edifices have been recognized. Volcanic shields (vs) are very large constructional forms with rough, concave slopes that become both convex (near the summit) and complex are capped by calderas (Fig. 10). The largest, Nix Olympica, is about 600 km across and may be on the order of 10 km high judging from the preliminary heighting data of other experiments. Volcanic domes (vd) are smaller and have smooth convex slopes and summit calderas (Fig. 11). Volcanic cones (vc) are low, broad, smooth-rimmed structures with large, flat-floored, generally circular summit craters (Fig. 12).

Deposits occupying two types of narrow depressions have been mapped as a composite unit, channel and canyon deposits (ch). The channels are incised curvilinear to sinuous features that commonly have a braided pattern and are flanked by terraces along parts of their courses (Fig. 13a). The canyon deposits consist of materials that fill the relatively flat floors of the 3–5 km deep east–west trending canyon system. The canyon deposits are locally hummocky and lack braided textures (Fig. 13b).

One of the most extensive units is the smooth plains (sp). At A-camera resolutions (approx 1–2 km) the unit shows little or no textural detail except for a few small craters and complex light and dark streaks, many of which appear to emanate from craters. B-camera pictures (approx 100–200 m) show a variety of surface features including multiple lobate scarps, pits and hollows, and complex furrows and ridges. The unit generally lies in large depressions of irregular shape. Some areas that appear to be smooth plains (particularly outside the equatorial region) may in fact be other terrain obscured by atmospheric dust.

The remaining units are all characterized by rough textures that appear to result from various deformational patterns. The chaotic terrain (ct) consists mostly of a jumbled array of sharp rectilinear blocks and slabs (Fig. 14). As described by Sharp *et al.* (1971), it has formed at the expense of surrounding geologic units. Some patches appear to lie at the head of braided channels; others occur within enclosed irregular depressions or craters. The fractured plains (fp) includes area of closely spaced, long, narrow linear graben and horsts along with areas where the fracture pattern appears coarser, somewhat more subdued, and locally reticulate to radial (Fig. 15). The grooved terrain (gt) consists of patches elevated above the surrounding plains characterized by a closely spaced network of partly sinuous grooves and ridges (Fig. 16). The most prominent occurrences surround Nix Olympica and may be related to this large volcanic shield.

The last three units, lineated terrain (lt), mountainous terrain (mt), and knobby terrain (kt) appear to surround large, generally circular basins, some of which, such as Hellas, lie just outside the mapped region. The lineated terrain (lt) is generally characterized by large, subdued scarps, or sharper-appearing ridges and grooves that are radial to the basins (Fig. 17a, b). The mountainous (mt) consists of large, widely spaced multipeaked mountains or massifs that are vaguely to strongly elongate; the flanks of some massifs are faceted and gullied (Fig. 18). The knobby

terrain (kt) consists of patches of closely packed, small sharp-appearing peaks (Fig. 19).

Small, closely spaced furrows, depressions, or channels, many with a dendritic pattern, appear to be superposed features with a distribution somewhat independent of the mapped geologic units (Fig. 20). They do not represent a discrete geologic unit but areas in which they are prevalent are indicated by heavy dotted lines. This furrowed terrain is not as extensive as shown in the southwestern part of Fig. 1. Its distribution is difficult to map because of the varying resolution of individual frames.

CRATERING AND CIRCULAR BASINS

Mariner 4, 6, and 7 photographs suggested that most of Mars was highly cratered, like the Moon's southern highlands and far side. Although Mariner 9 has revealed extensive relatively uncratered regions, cratering still appears to have been the dominant geologic process in approximately 40% of the equatorial region and in much of the area outside the map. Martian craters grossly resemble lunar craters of comparable size and most of the differences between them can be attributed to greater degradation. An unexplained feature seen in B-frame pictures of many craters is the presence of a lobate scarp or even a raised rampart at the outer margin of the rim deposit. Secondary crater fields around large craters have not been positively identified and bright rays are certainly absent. Isolated chains and clusters of small craters seen in some B-frames may be secondary craters, but they are not associated with an obvious primary crater. We believe that, as on the Moon, the majority of the craters are of impact origin as indicated by their morphologies and the slope of their size-frequency distributions. An unknown but probably small fraction is almost certainly of volcanic origin, but it is very difficult to distinguish individual volcanic craters from impact craters when both are severely degraded.

Circular basins complete the series of craters at the upper end of the size range.

Some of these appear to have multiple rims, although the outer rims are not as well developed as around the fresher lunar basins. Four basins have been identified in the equatorial region. The largest Martian basin is Hellas, about 2000 km in diameter. Only the northern part of the rim lies within the map area, forming an arcuate belt of rugged, multipeaked, generally elongate mountains mapped as mountainous terrain between longitudes 260° and 310° and south of latitude 20°S. This terrain resembles the Montes Apeninus chain that forms the rim of the Imbrium basin, which with a diameter of 1500 km is the largest basin on the Moon. The second-largest basin is here named the "Libya basin" for the telescopic feature that coincides approximately with the most conspicuous segment of its main ring. This mountain arc (Fig. 3), which extends along the equator between longitudes 260° and 285°, resembles the Hellas ring and is portrayed by the same map unit (mt). Judging from its trend and from that of several concentric graben (Figs. 3 and 4), this ring probably arcs around northward to continue as the knobby terrain mapped northeast of Syrtis Major. A conspicuous and sharply bounded outer scarp of the Libya basin arcs from latitude 10°S, longitude 270° to latitude 0°, longitude 295°. Extensive basin-filling plains deposits (cp and sp) occur within the map area north of the equator between longitudes 200° and 290°. These plains fill both the central Libya basin and extensive tracts west and east of it, occupying either depressions concentric with the basin or other, older basins that are now hidden; both situations have lunar analogs.

The two smaller basins are named for the features Edom, near 340°W and the equator, and Iapygia, near 305°W and 15°S. The Edom basin has a conspicuous outer scarp and both basins have inner and outer rings that appear as gentle highs. Conspicuous radial fractures and flat-bottomed troughs, partly filled by cratered plains, in lineated terrain (lt) southwest of the Iapygia basin, are much like the radial structures around lunar basins, though less conspicuous and extensive.

These smaller basins are comparable in size to the Crisium basin on the Moon.

VOLCANISM

One of the most significant Mariner 9 results is the recognition of the major role of volcanism in the formation of the surface of Mars. The most striking of the volcanic features are the four enormous shield volcanoes of the Tharsis-Amazonis-Elysium region each of which is at least twice as massive as the largest comparable features on Earth. South Spot and Middle Spot have simple, circular, summit calderas whereas Nix Olympica and North Spot have composite calderas consisting of several intersecting craters with floors at different levels. The floors are generally smooth and very sparsely cratered. A series of concentric arcuate graben lie outside the central caldera on South Spot (Fig. 21) and Middle Spot. The flanks of the shields are marked by radially elongate and overlapping lobes that form an intricate surface pattern. High-resolution photography of the flanks of Nix Olympica shows that the surface is made up of many narrow elongate ridges roughly radial to the central crater (Fig. 22). Along one large ridge is a narrow channel suggestive of a lava channel or a collapsed lava tube. The flank pattern generally fades out into the surrounding plains but at Nix Olympia terminates at an abrupt escarpment at the base of the shield. The martian volcanic shields have no lunar analogs but are strikingly similar to some terrestrial volcanoes, for example, Fernandina in the Galapagos Islands (Simkin and Howard, 1970).

A distinctive volcanic shield lies in the cratered terrain of Mare Tyrrhenum (253°W, 22°S). The central crater is approximately 20 km across and has a smooth floor. The rim within one crater diameter of the edge of the crater is also smooth, but beyond that low ridges and narrow sinuous channels extend approximately 200 km radially away from the crater to give the structure a flowerlike appearance and the informal name of "The Dandelion." The channels around the crater resemble some

isolated channels that occur elsewhere in the cratered terrain and raise the possibility that these also may be volcanic.

Volcanic domes also occur mainly in the Tharsis region. These generally have a central caldera one-half to one-third the diameter of the dome. The flanks of the domes are convex upward and appear smooth in the low-resolution A-frame pictures. In the high resolution B-frames numerous radial channels are visible, some terminating in shallow depressions. The domes and the channels terminate abruptly against the surrounding plains.

In the same region as the domes and shields are several craters that are low-rimmed but morphologically distinct from craters typical of the general crater population; they are interpreted as volcanic craters (vc). These craters have a simple circular outline or cuspatate walls. The rims are smooth, narrow, and simple in outline, and end abruptly against the surrounding terrain, contrasting markedly with the rough, hummocky surface texture and stellate outlines of impact crater rims.

The striking edifices radially symmetric about a central vent are not the only probable volcanic features observed on Mars. Some of the plains, apparently featureless in A-frame pictures, appear in B-frames to have low ridges and hills, or finely lobate escarpments suggestive of flow fronts. These fronts strongly resemble those of the flows in Mare Ibrium on the Moon. Such features are particularly common in the south, in the region near the volcanic shields suggesting that much of the smooth plains in these areas is formed by extensive lava flows (Fig. 23). Moreover, it is possible that the grooved terrain (gt) occupying much of the area around Nix Olympica consists of deeply eroded volcanic flows that belong to the outer zone of Nix Olympica or even to older volcanic constructs.

CANYONS

The discovery of the equatorial canyon system of the Coprates region was another startling Mariner 9 result. The canyon

system consists of a series of roughly parallel steep-walled, linear depressions that range from 1 to 3 or more km in depth with an average width of about 100–150 km and an overall length of more than 2500 km. In the Melas Lacus region the main canyon widens to about 250 km. Here two large roughly rectilinear troughs border the main canyon so that the total width is on the order of 500 km.

The canyon walls are rarely smooth, but exhibit a variety of re-entrants, ranging from alcoves with gently curved broad outlines to a complex branching system of ravines with steep gradients (Fig. 24). In addition, large gullies, some of which have a dendritic tributary pattern, extend backward from the canyon walls for as much as 150 km. Hummocky terrain which appears to be landslide debris occurs at the base of some re-entrants, particularly in the open alcoves. The gullies and the ravines resemble in form those cut by running water on Earth. Many gullies show an orthogonal pattern suggesting structural control. Whatever originally formed the canyons, the present shape appears to be the result of slope retreat effected by processes the same as or closely analogous to those that widen terrestrial canyons: landsliding, debris flow, artesian sapping, and possibly erosion by running water.

Parallel to the main canyons and extending beyond the blunt ends of some troughs are linear chains of rimless pits (Fig. 25). At the head of the canyon system in the Noctis Lacus region (90–100°W longitude) is a labyrinth of elongate depressions and pits (Fig. 26). The canyons might have begun their development like the features of the Noctis Lacus region and were subsequently widened by erosion. The problem of disposal of materials from the canyon system is particularly vexing. Some debris may have been transported along the canyon system and out the east end (which is the low end) but features indicative of such transport are not evident. Transport over the surface, except by wind, is impossible in the case of entirely closed basins, such as one just north of the main canyon system in Tithonius Lacus (Fig.

27). An alternative hypothesis is that the canyons formed by collapse at essentially their present limits, and were later enlarged a small amount by slope retreat. This hypothesis also presents difficulties, as the boundaries are not obvious faults, and as movement of the same volume of material is required in the subsurface. The volume of the canyons is by rough estimate only twice the volume of the Nix Olympica shield, so that subcrustal mass movement in connection with magmatism is not unreasonable. We emphasize, however, that we have seen no evidence of a large-scale pattern of displacement corresponding to the global tectonics of Earth. Specifically, an analogy between the canyon system and terrestrial rift valleys, beyond the fact that both are extended depressions, has little to confirm or refute it.

CHAOTIC TERRAIN

Chaotic terrain is most abundant in the region to the east of the main canyon system ($15\text{--}30^\circ\text{W}$ longitude) where it occurs in numerous isolated large patches. It appears to result mostly from the withdrawal of materials in the subsurface and the consequent collapse of the overlying strata. The parts of this unit that are adjacent to broken, fresh-appearing scarps could be the result of headwall sapping which has initiated downward sliding and the concomitant breaking up of the bedrock into large angular slabs and blocks. Structural failure in these areas appears to be controlled by a pre-existing fracture pattern. Many large patches of chaotic terrain, particularly those at lower elevations than the surrounding terrain, are disaggregated into multitudinous small blocks, many of which approach the limit of TV resolution. Some of these patches, such as those in the region of $20\text{--}25^\circ\text{W}$ longitude lie entirely within moderately cratered terrain (mc). Roof caving appears to be the most adequate explanation for these patches. Roof caving, headwall sapping, and slumping probably operated both separately and sequentially in different areas to produce chaotic terrain.

CHANNELS

Many of the channels seen on the accompanying maps are remarkably similar to fluvial channels on Earth. These sinuous multichannel features with their discontinuous marginal terraces contain teardrop-shaped islands and channel bars (Fig. 28) must have been carved by running fluids. The current working hypothesis is that the fluid was water, although the possibility of erosion by fluidized solid-gas systems must also be considered. Integrated drainage systems like those of established river systems on Earth, composed of small channels that successively join to form wide channels of higher order and that culminate in a master channel, are markedly absent. The Martian channel systems, most of which show little change in character from head to mouth, resemble features produced by episodic floods on Earth—ephemeral channels on desert fans or, on a scale more nearly approaching the Martian channels, the channels cut by catastrophic draining of ice-dammed lakes or the melting of ice by subglacial volcanism. Braiding, evident in many channels, is indicative of a strongly varying flow regime, in which the stream during the waning stages of a flood is unable to transport the sediment carried during peak flow.

A source must be found for the enormous quantities of water (or other fluid) that carved the channels, some of which are over 200 km wide and 1500 km long. Theoretical considerations (Murray and Leighton, 1966) suggest that the Martian atmosphere could never have produced the volumes of water necessary, although an adequate quantity of water episodically released from the polar caps has been conjectured (Sagan, 1971). The source of the fluids could be lithospheric rather than atmospheric. Of particular significance is the apparent relation between the braided channel deposits and the chaotic terrain in the Margaritifer Sinus region (Fig. 14). Some of the largest channels appear to originate in patches of chaotic terrain and flow northward into the Chryse region. The following tentative model is proposed.

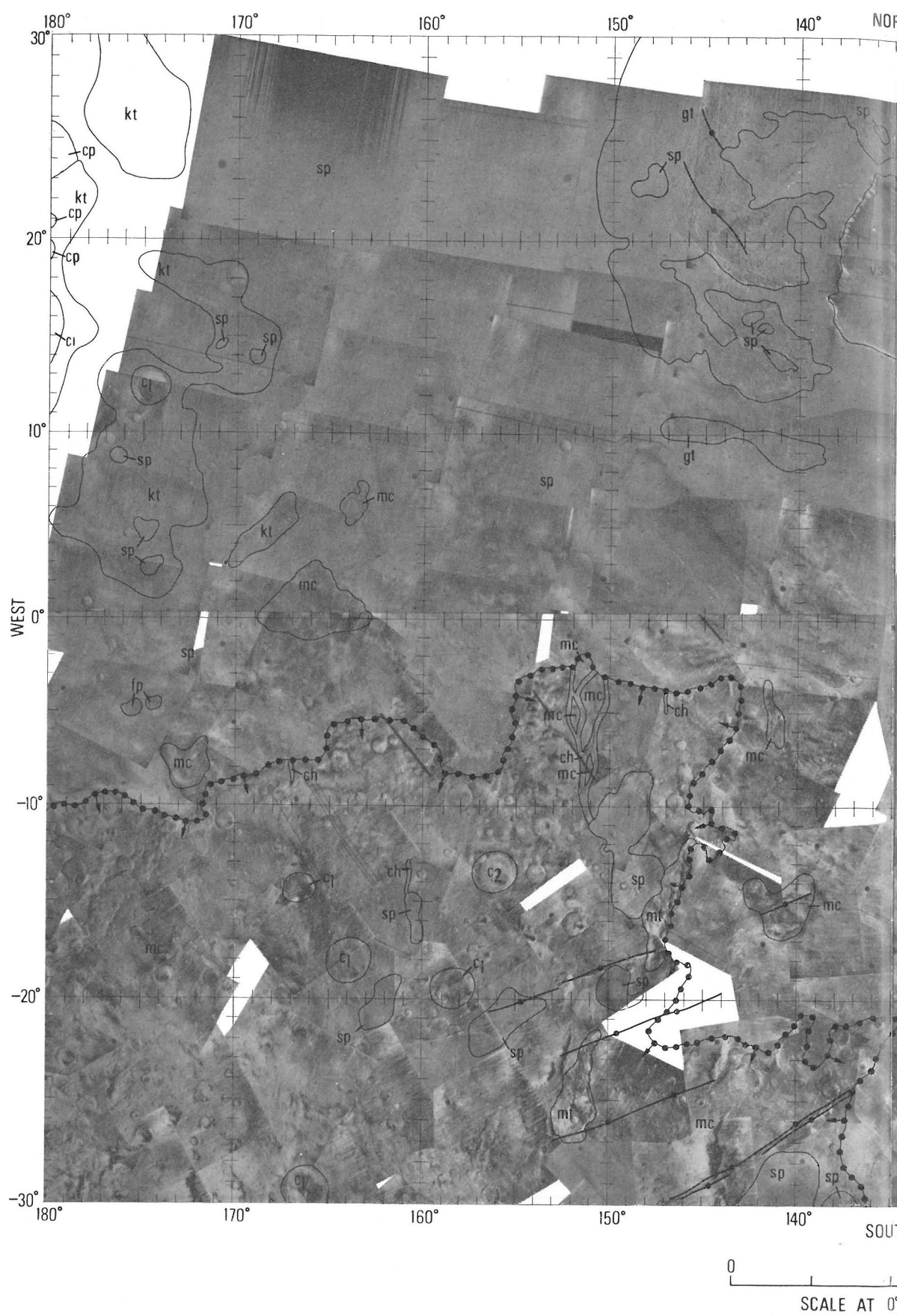
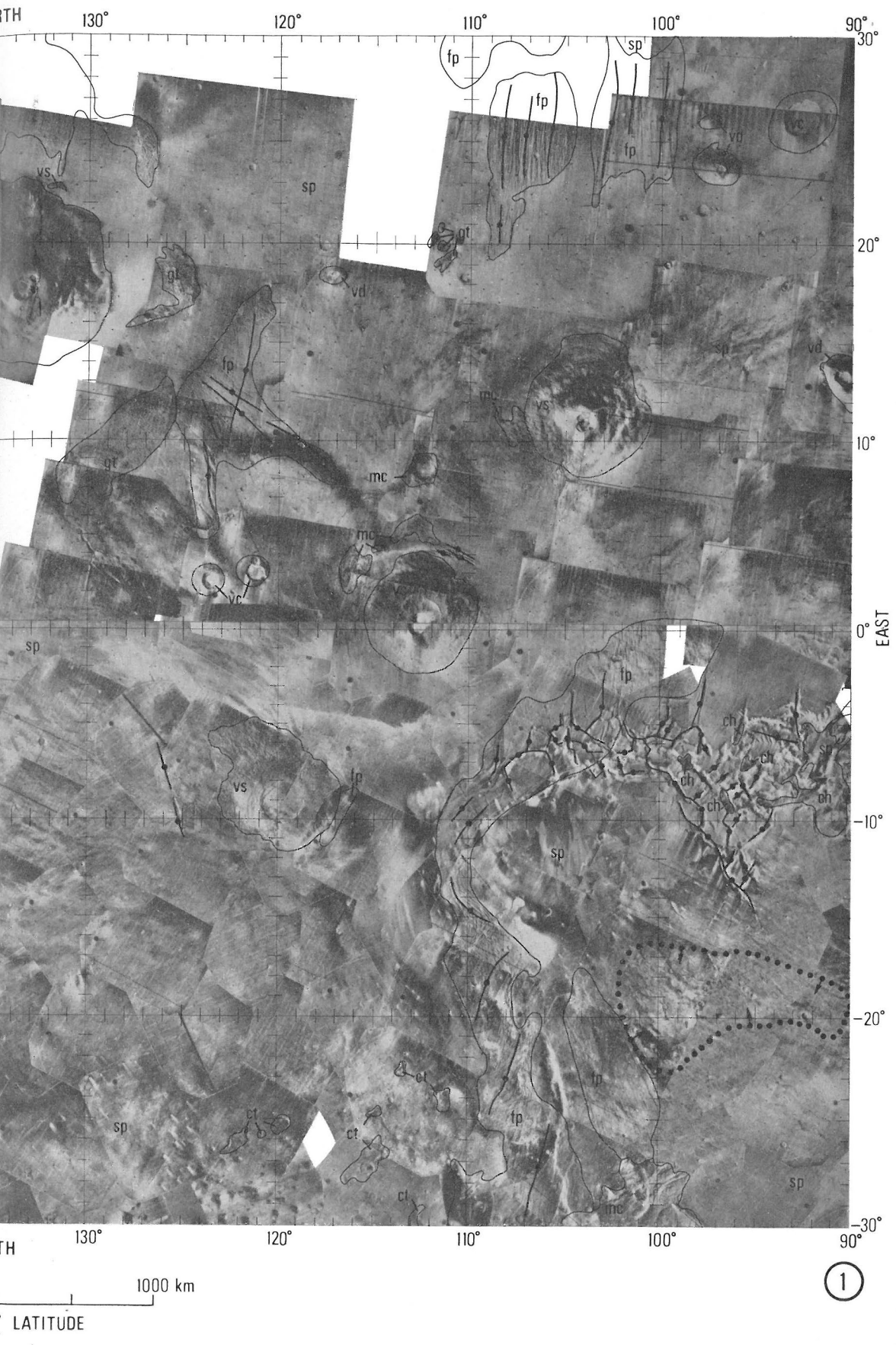


FIG. 1. Preliminary geologic map of part of the



The equatorial region of Mars by M. H. Carr.

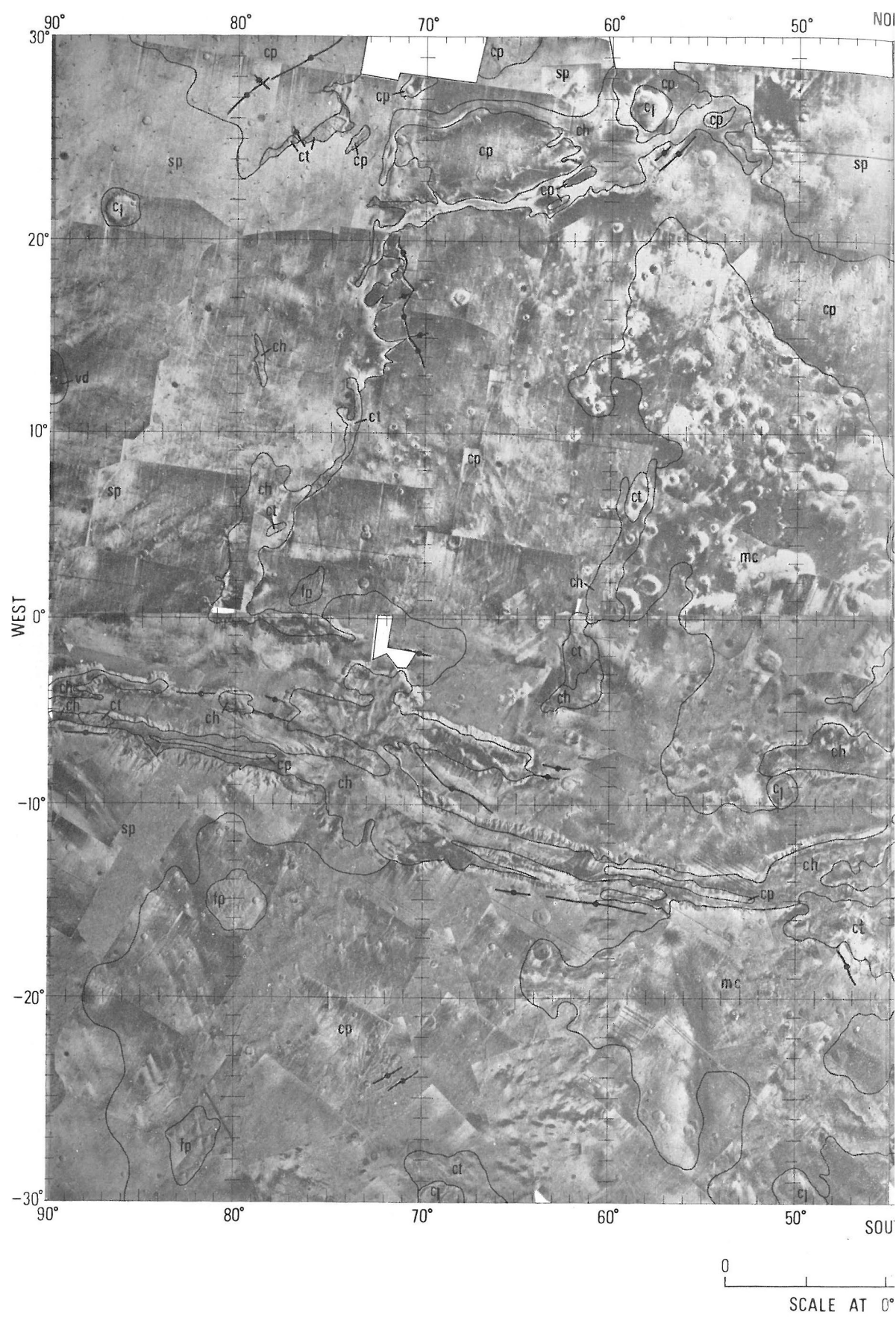


FIG. 2. Preliminary geologic map of part of the



the equatorial region of Mars by J. F. McCauley.

(2)

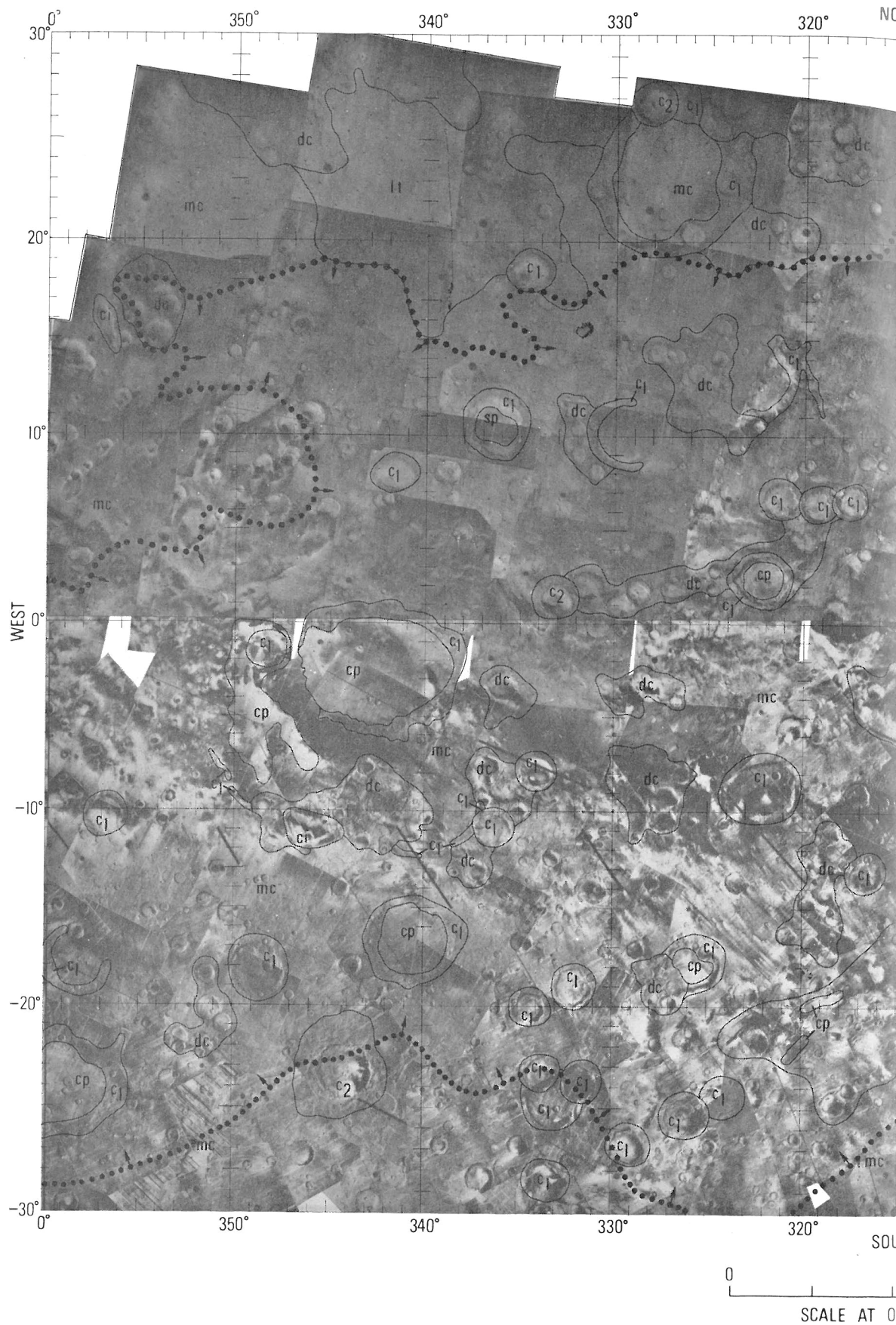


FIG. 3. Preliminary geologic map of part of the



equatorial region of Mars by D. E. Wilhelms.

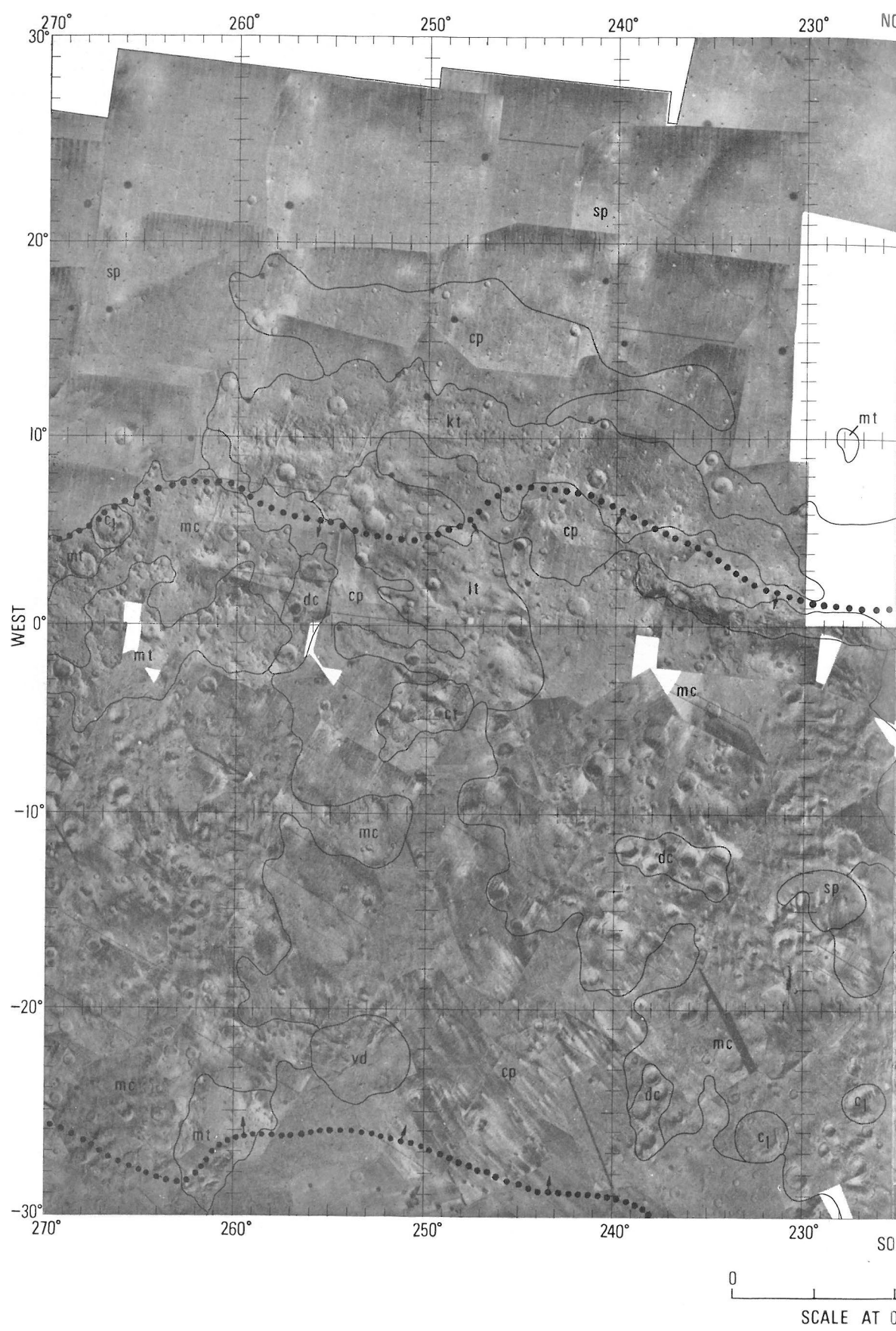
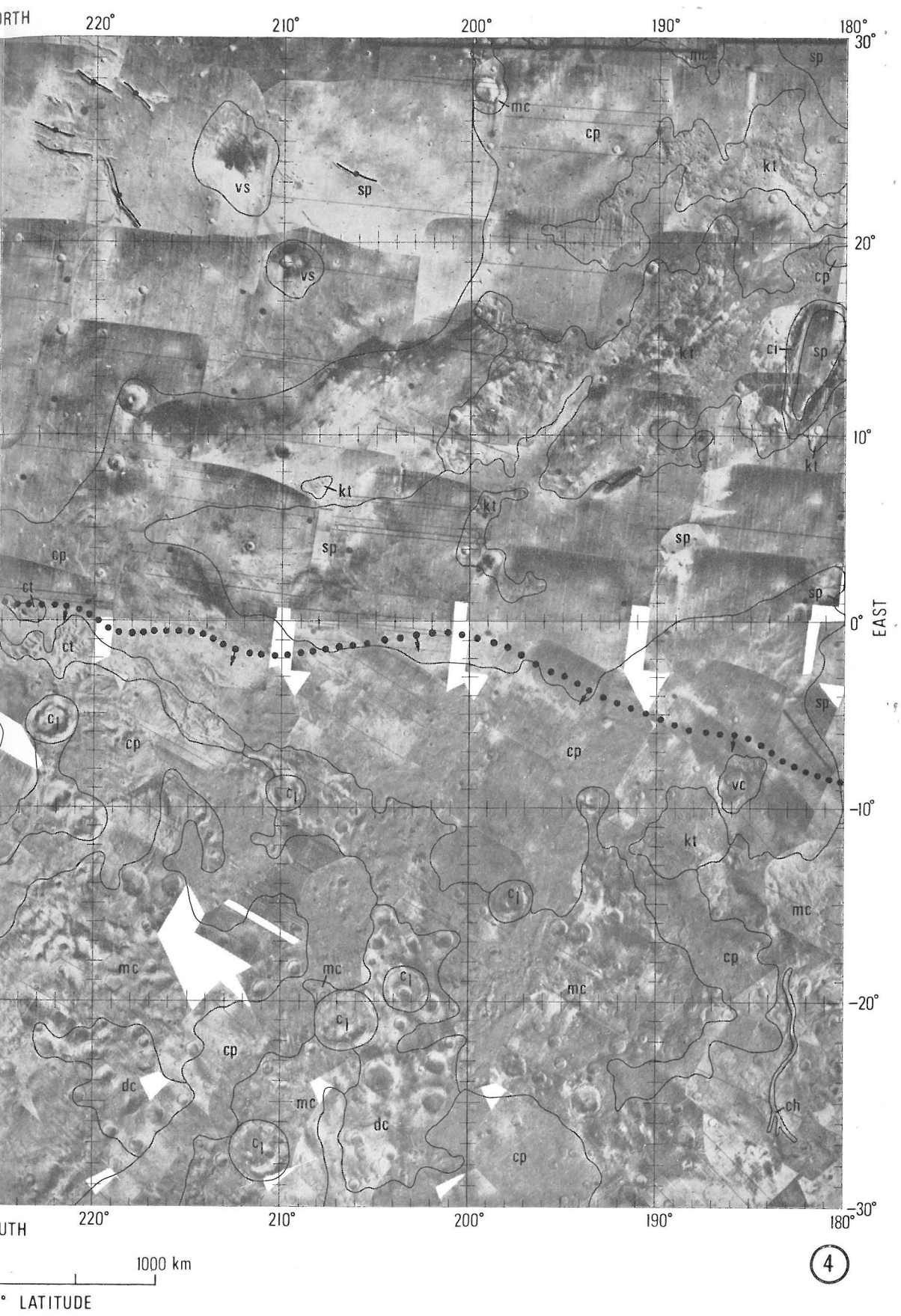


FIG. 4. Preliminary geologic map of part of the Moon's surface.



The equatorial region of Mars by D. J. Milton.

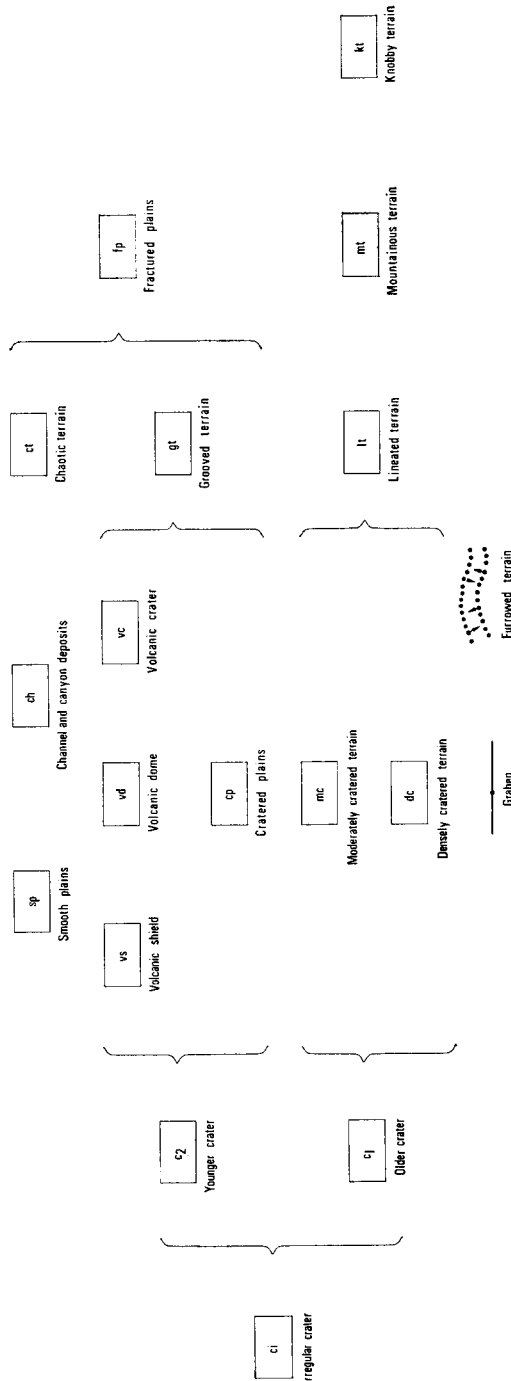


FIG. 5. Explanation of the preliminary geological map of the equatorial region of Mars.

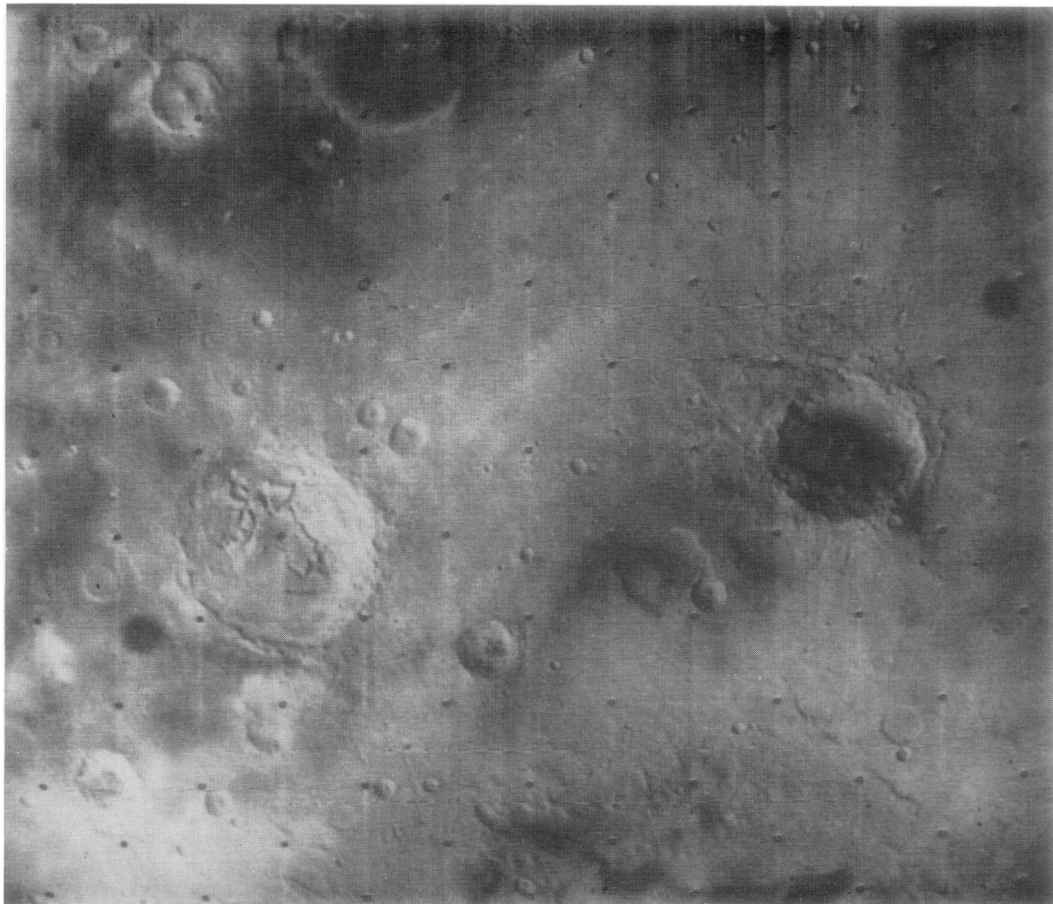


FIG. 6. The right-hand of the two large craters, 70 km in diameter and not mapped separately, is the type example of the younger crater unit (c_2). It is sharp-appearing, relatively deep, and has an ejecta blanket whose rough texture is visible out to one crater diameter in some sectors. A small central peak is visible. At the bottom of the picture note also the rough arc of terrain which is the northern rim of the Edom basin. A continuum of crater types can be recognized in this picture, ranging from the subdued irregular depression at the top left, through the large degraded and broken-floored crater left of center, to progressively sharper but smaller scattered craters. The dimension across the top of each A-frame is about 400 km. A-frame 4181-60, centered at 3°N, 304.5°W. North at top of this and all succeeding pictures.



FIG. 7. Type example of the irregular crater unit (ci), a 380-km long rough-rimmed depression which resembles the lunar crater Schiller. This structure is larger and appears rougher than Schiller. Coalescing circular segments do not account for its general shape; its origin remains uncertain. From uncontrolled A-frame mosaic; crater centered at 14°N and 181.5°W.

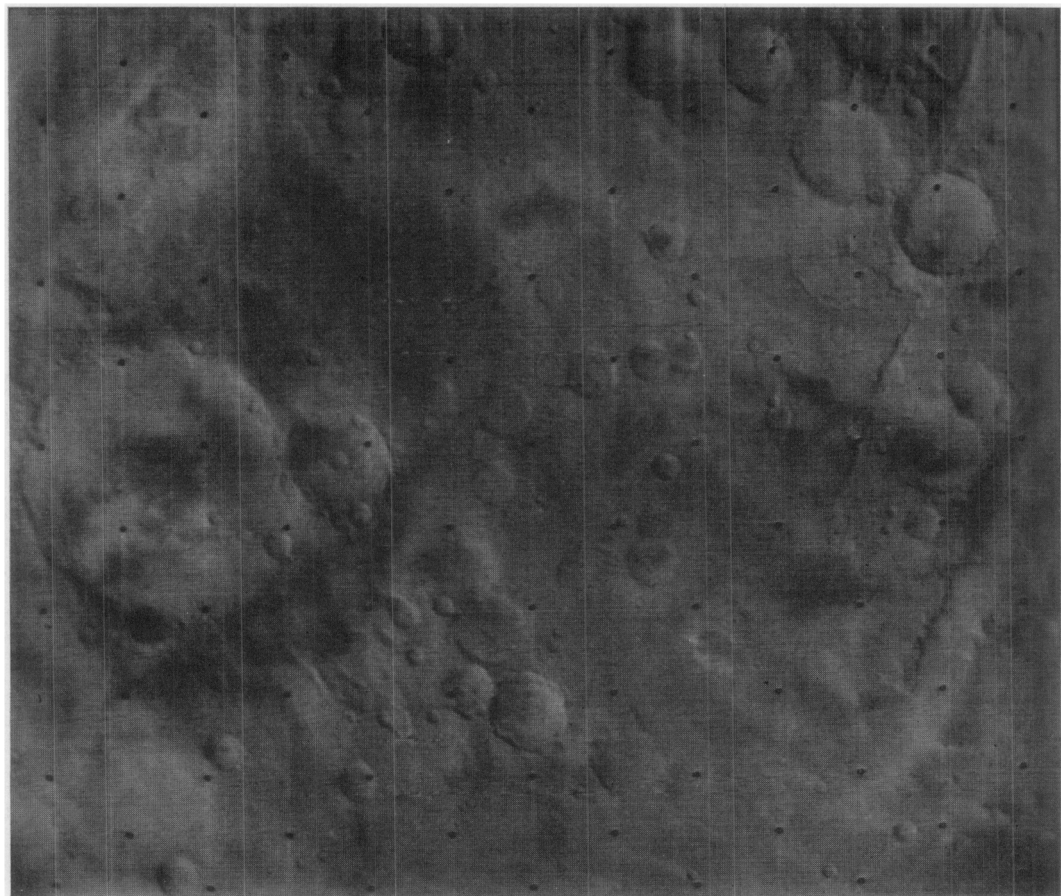


FIG. 8. Type areas of densely cratered terrain, moderately cratered terrain, and older craters. Densely cratered terrain (dc) includes the closely spaced large craters in middle left and upper right of the picture with relatively rough terrain between and adjoining the craters. The largest crater is about 190 km in rimcrest diameter and is the type example of the older crater unit (e_1). The remaining terrain in the picture is the moderately cratered unit (mc). Its craters are smaller and more widely spaced, probably because the undulatory intercrater material has buried the large old craters everywhere except in the island-like patches of densely cratered terrain. Note also the parallel troughs in the right part of the picture. These are concentric with the Libya basin and presumably formed by faulting after the basin formed. A-frame 4183-90, centered at 22.5°N and 289.5°W .



FIG. 9. Type area for cratered plains unit (cp). Note scattered nature of moderately sharp 30–50-km craters, and its tendency towards a darker albedo. Large lunar mare type ridges seen to the south just off picture. B-camera frames in this area show numerous small, fresh-appearing lobate ridges. From uncontrolled A-frame mosaic centered near 15°N and 65°W.

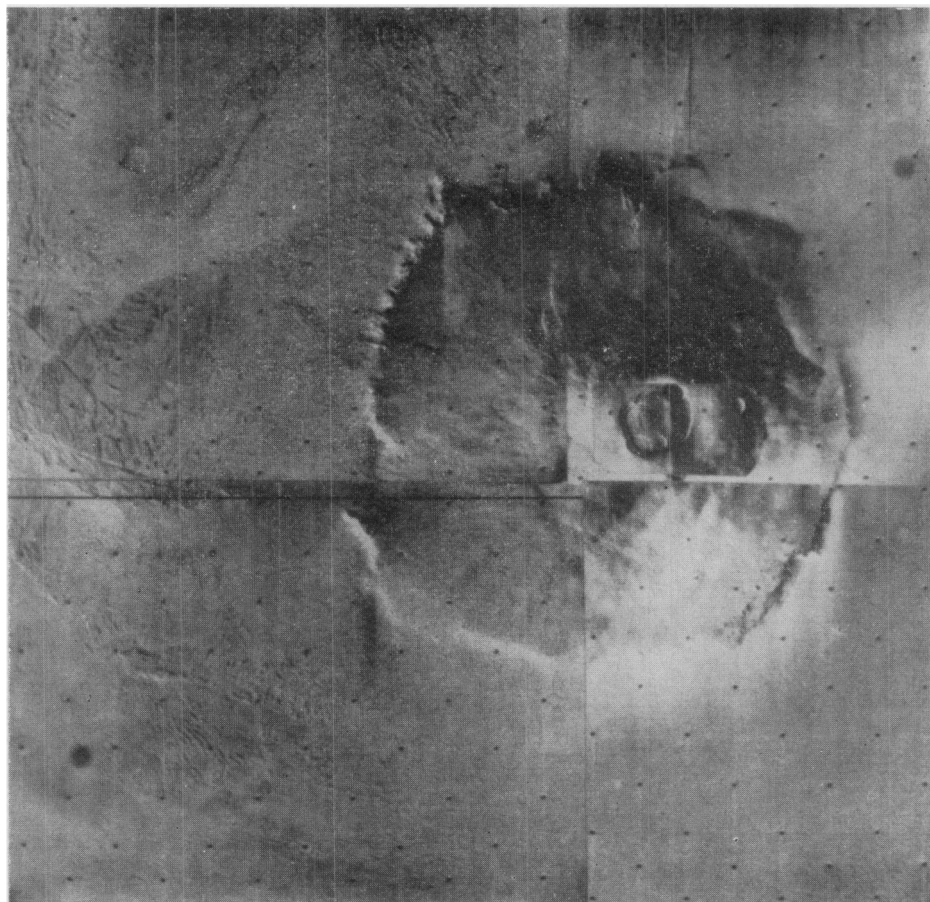


FIG. 10. Volcanic shield of Nix Olympica. The shield (unit vs), approximately 600 km across, slopes gently away from the central crater and is surrounded by a peripheral escarpment. The central crater is multiple, consisting of several intersecting circular depressions with level floors. Smooth plains (unit sp) in lower right corner of picture. Grooved terrain surrounding Nix Olympica at left of picture (unit gt). A-frame mosaic centered at 18°N and 137°W.

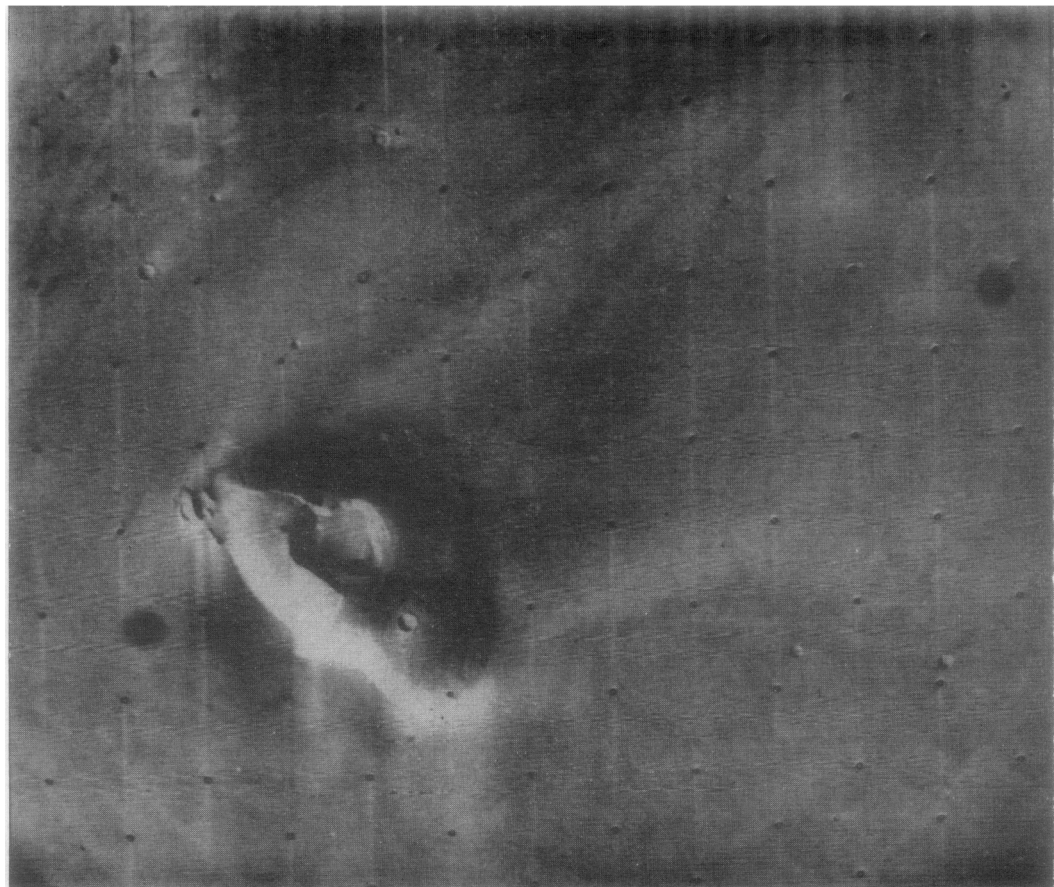


FIG. 11. Volcanic dome in the Tharsis region. The dome (vd) is approximately 120 km across and has smooth convex upward flanks. The central crater is multiple and has a flat floor and steep walls with several terraces. The flank of the dome appears to have been faulted. Smooth plains (sp) with light and dark streaks surround the dome. A-frame 4189-72 centered near 16°S and 88°W.



FIG. 12. Volcanic crater in the Tharsis region. The crater is approximately 40 km across and has a level floor, steep walls, and a smooth sharply demarcated rim. The crater on the north rim is probably of impact origin; it has the hummocky rim, central peak, and complexly terraced walls typical of some lunar and terrestrial impact craters. The crater is surrounded by smooth plains (sp). A-frame 4182-60 centered near 3°N and 120°W.

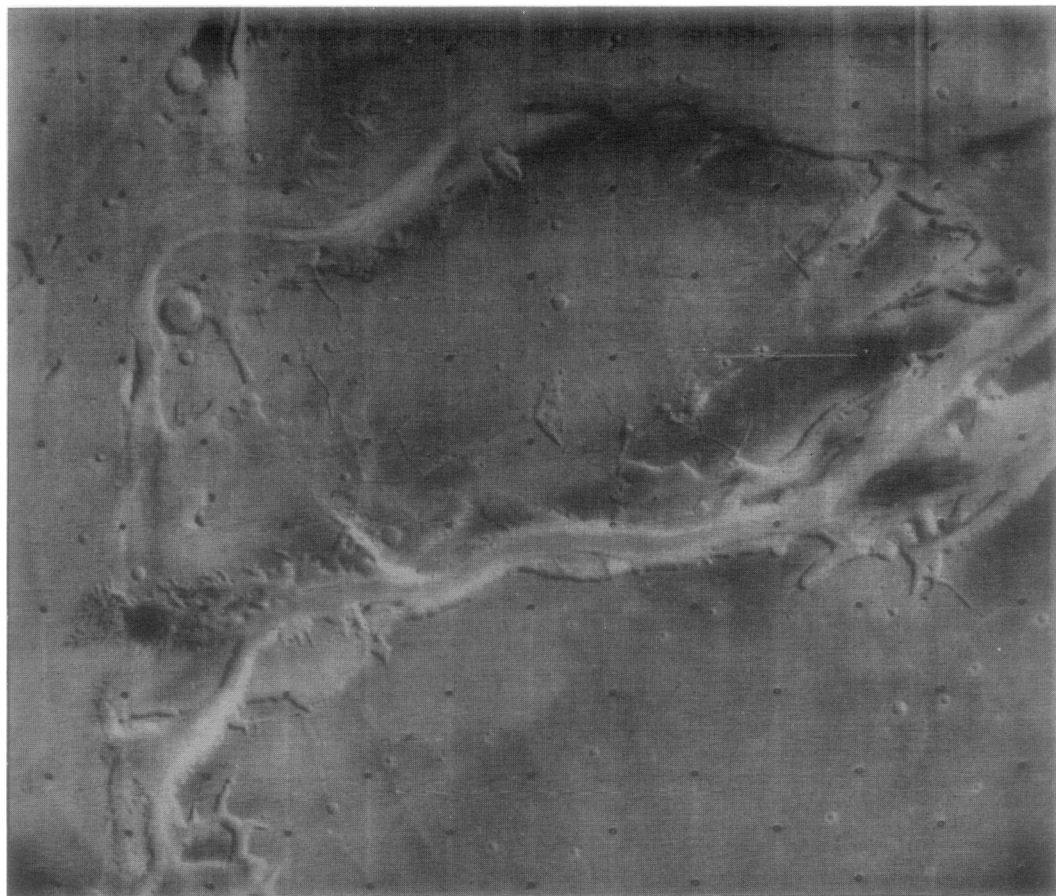


FIG. 13a. Type area of channel deposits within erosion valleys. Note the terraces along part of the course of the southmost channel and the remnant islands at its eastern end. Fracturing locally controls the channel course. In the lower left center an incipient dendritic pattern can be seen which appears to represent the most recent erosional episode. The gently meandering channel at the north of the picture appears to be partly obscured by younger smooth plains (sp), whereas parts of the more southerly channel are incised into the plains. A-frame 4193-84 centered near 21°N and 69°W.

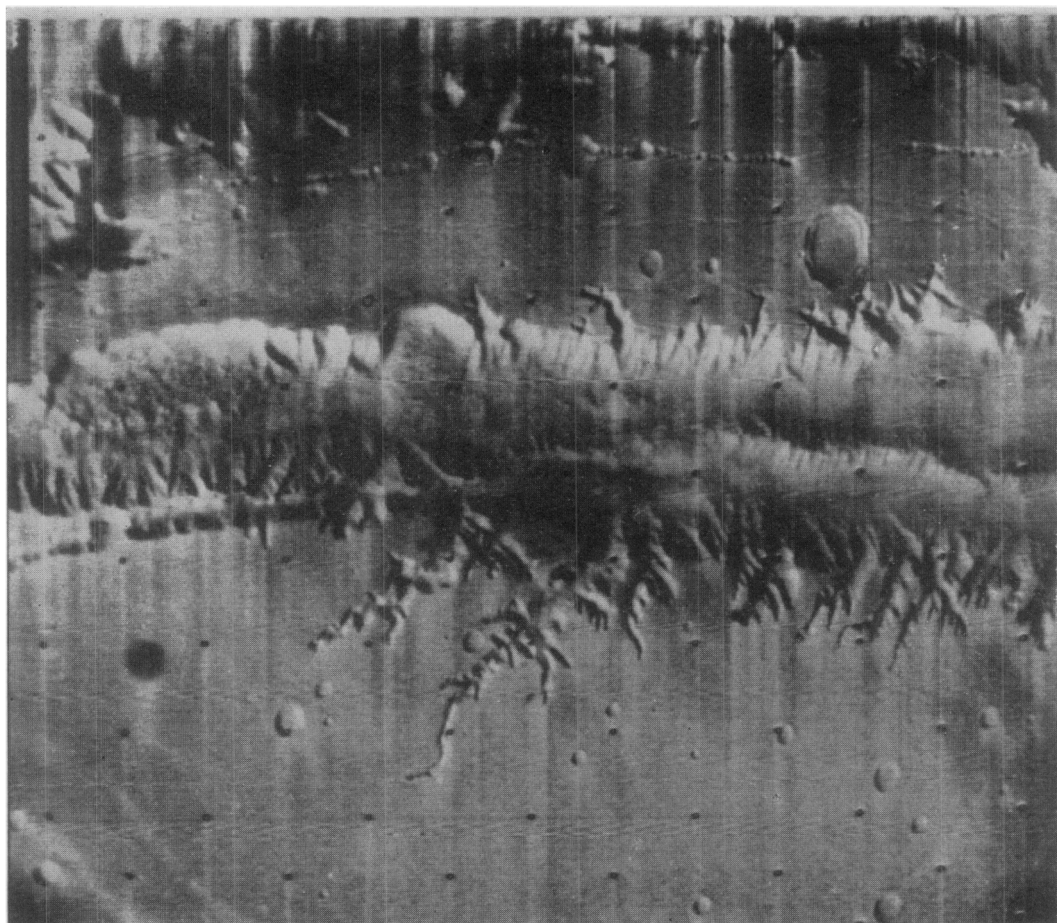


FIG. 13b. Canyons, erosional tributaries, and canyon floor deposits; east-west dimensions of canyon about 400 km, depth estimated to be about 2–3 km. Note fluted medial ridge extending from left center of picture and subsidiary trough at right center; gullies are controlled by an almost orthogonal fracture pattern. Hummocky material in canyon floor at west end of picture appears to be landslide debris; cusp on north wall near center is probably an erosional alcove and not a truncated crater. A-frame picture centered near 6°S and 85°W.

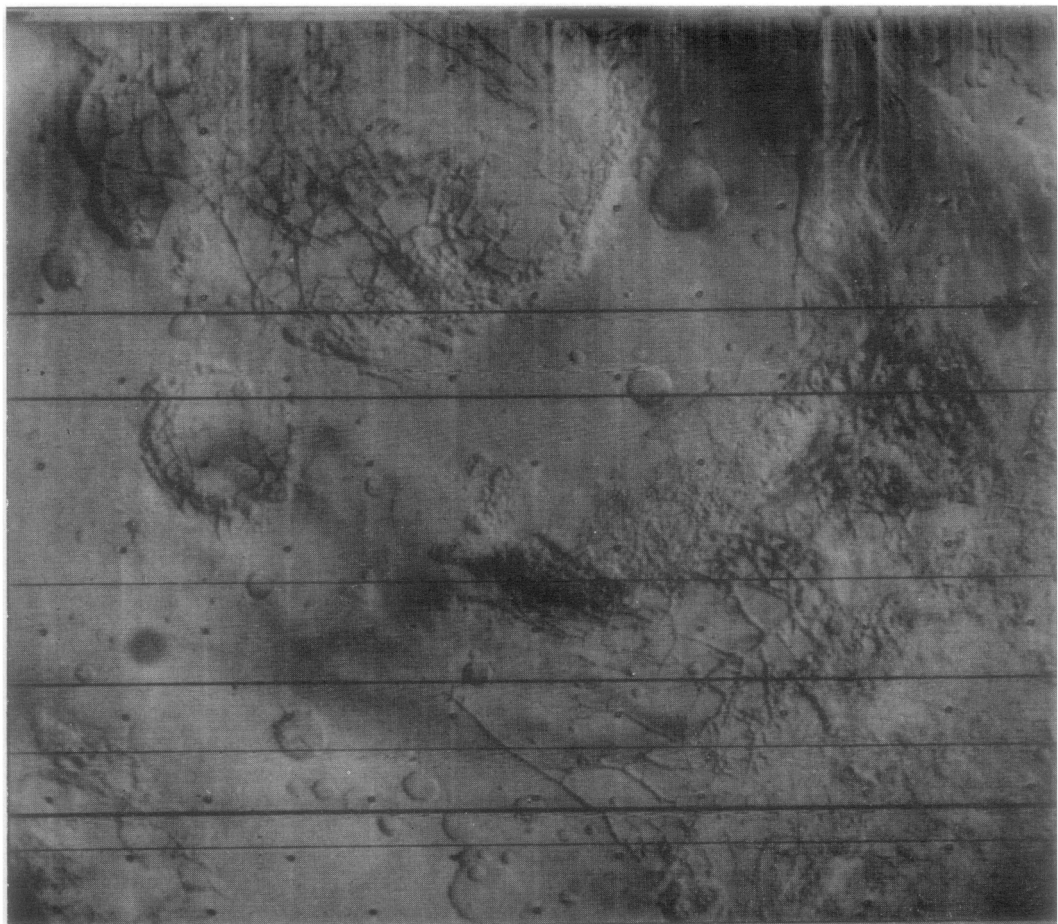


FIG. 14. Type area for chaotic terrain (ct). Unit consists of a complex mosaic of broken slabs and blocks that now lie generally below the surface of the surrounding units from which they formed. The breakup of older surfaces is locally so intense that individual fragments are near the limit of resolution. Note braided channel in upper right corner originating from patch of chaotic terrain in right center of picture. This particular channel extends for some 1500 km into the Chryse region. A frame 4206-57 centered at about 2°S, 20°W.

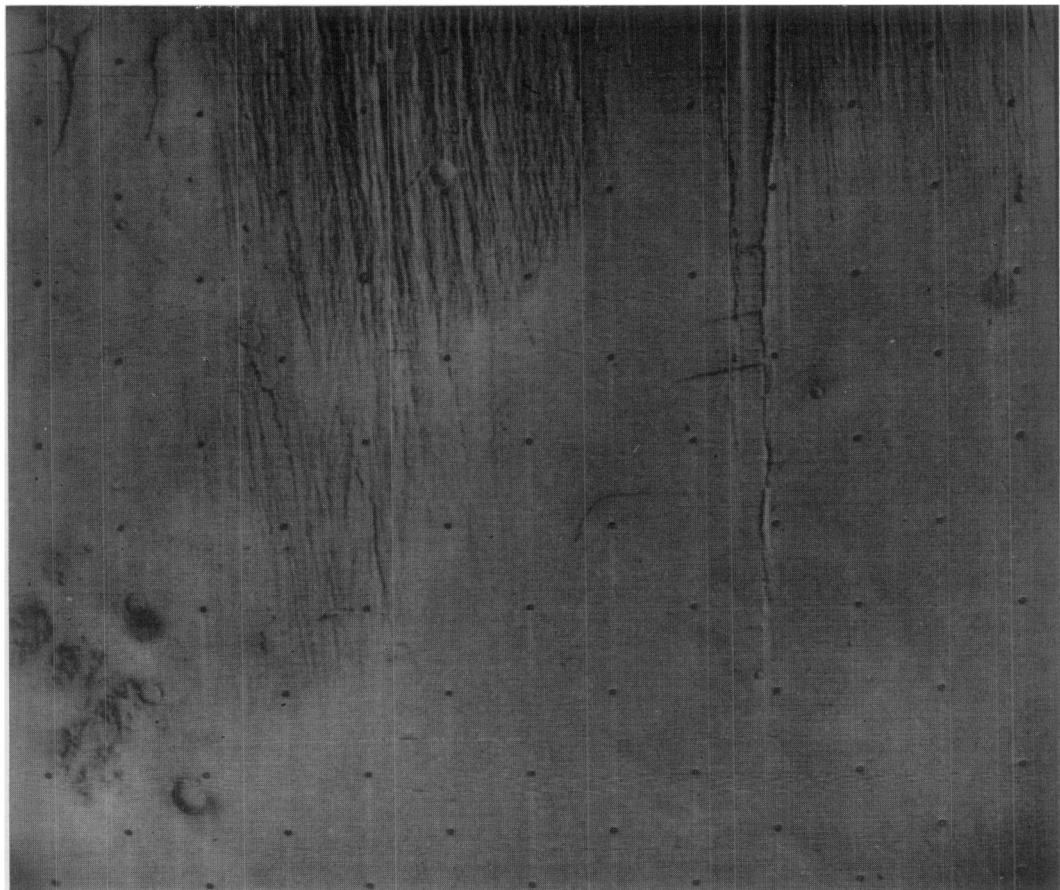


FIG. 15. Fractured plains (fp) north of Ascraeus Lacus. Unit consists of materials that are fractured along numerous closely spaced, subparallel, north-south trending faults. A-frame 4184-89 centered near 23°N and 107°W.

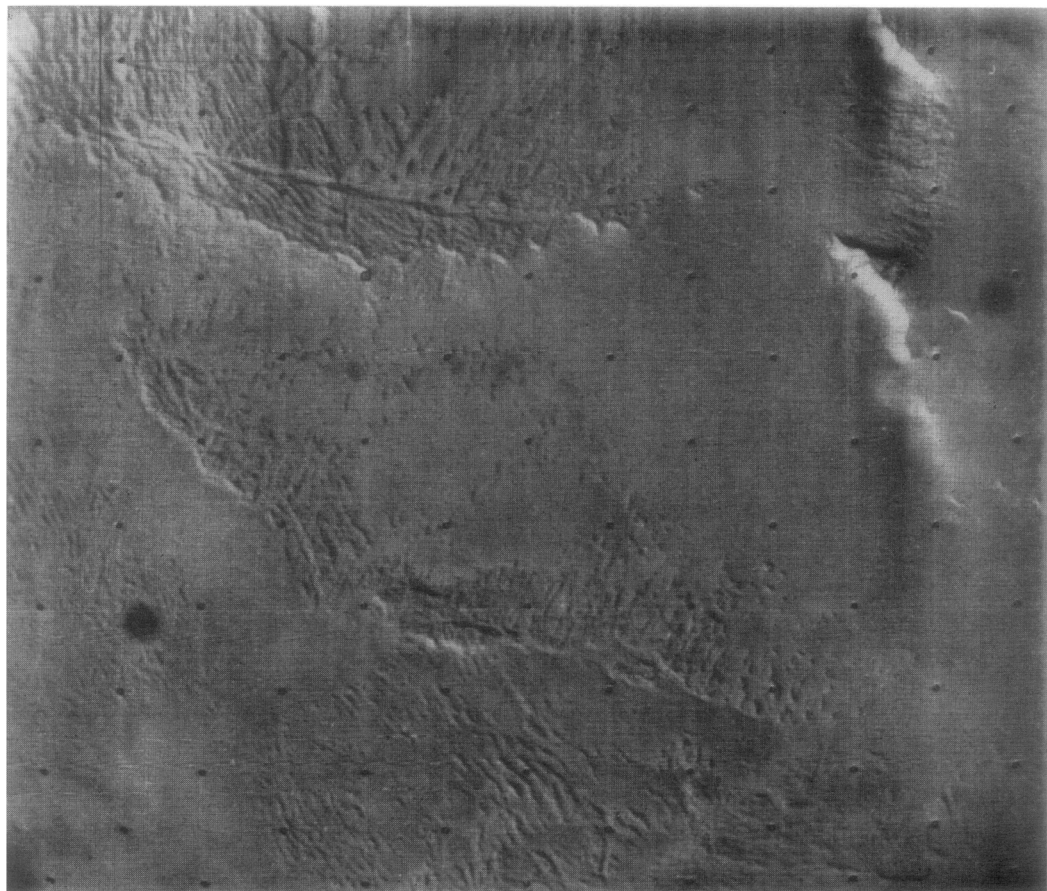


FIG. 16. Grooved terrain (gt) west of Nix Olympica. The grooved terrain consists largely of closely spaced low ridges and intervening linear troughs apparently faulted along arcuate fractures and tilted gently to northeast. The edge of Nix Olympica is at the NE corner of the frame. A-frame 4174-77 centered near 18°N and 140°W.

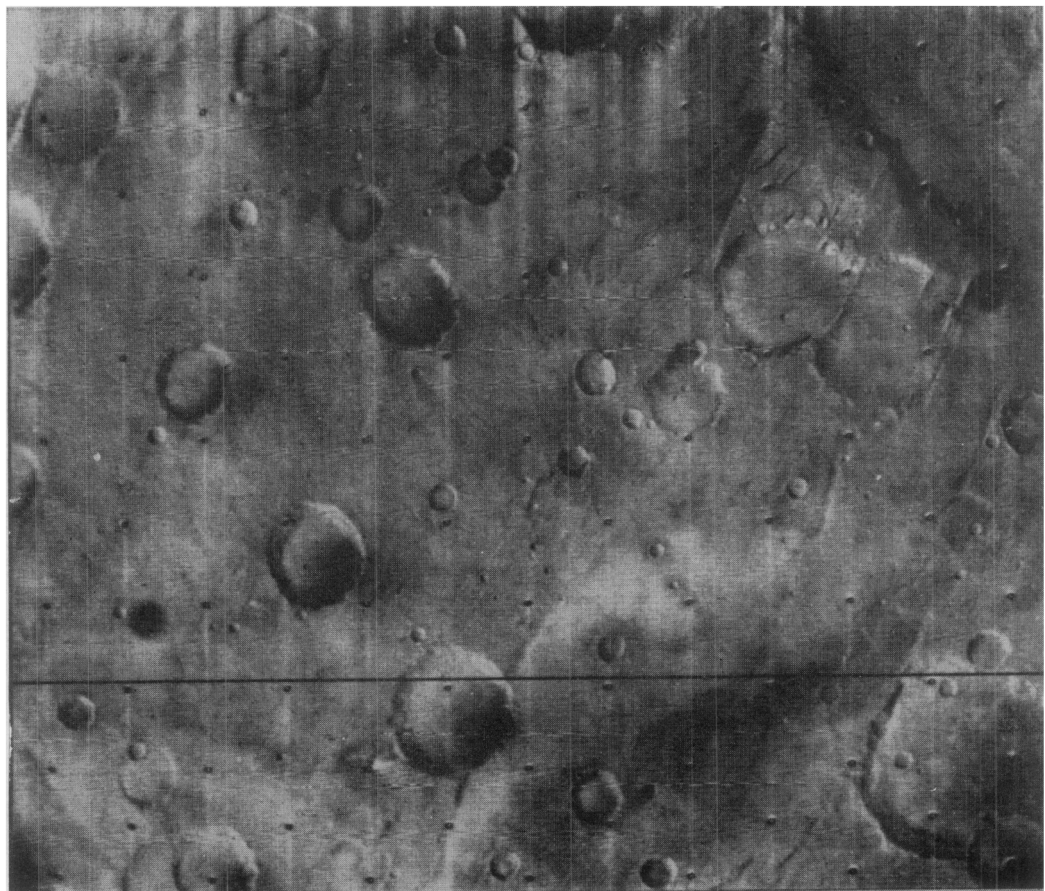


FIG. 17a. One variant of lineated terrain (lt) with grooves radial to Iapygia basin (upper right). A-frame 4181-33, centered at 15.5° S and 311° W.

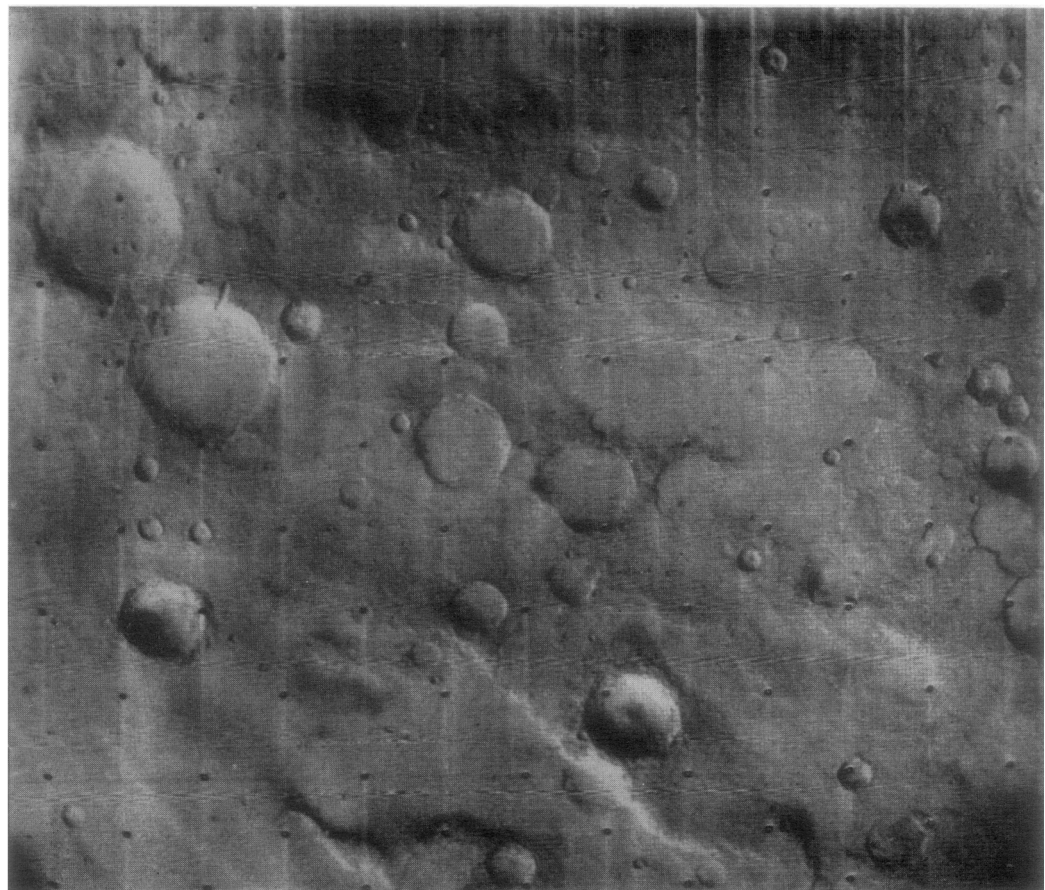


FIG. 17b. Second and more common variant of lineated terrain here consisting of a stepped surface with a series of plateaus and troughs radial to Libya basin (out of picture to upper left). A-frame 4194-60, centered at 5° N and 250° W.

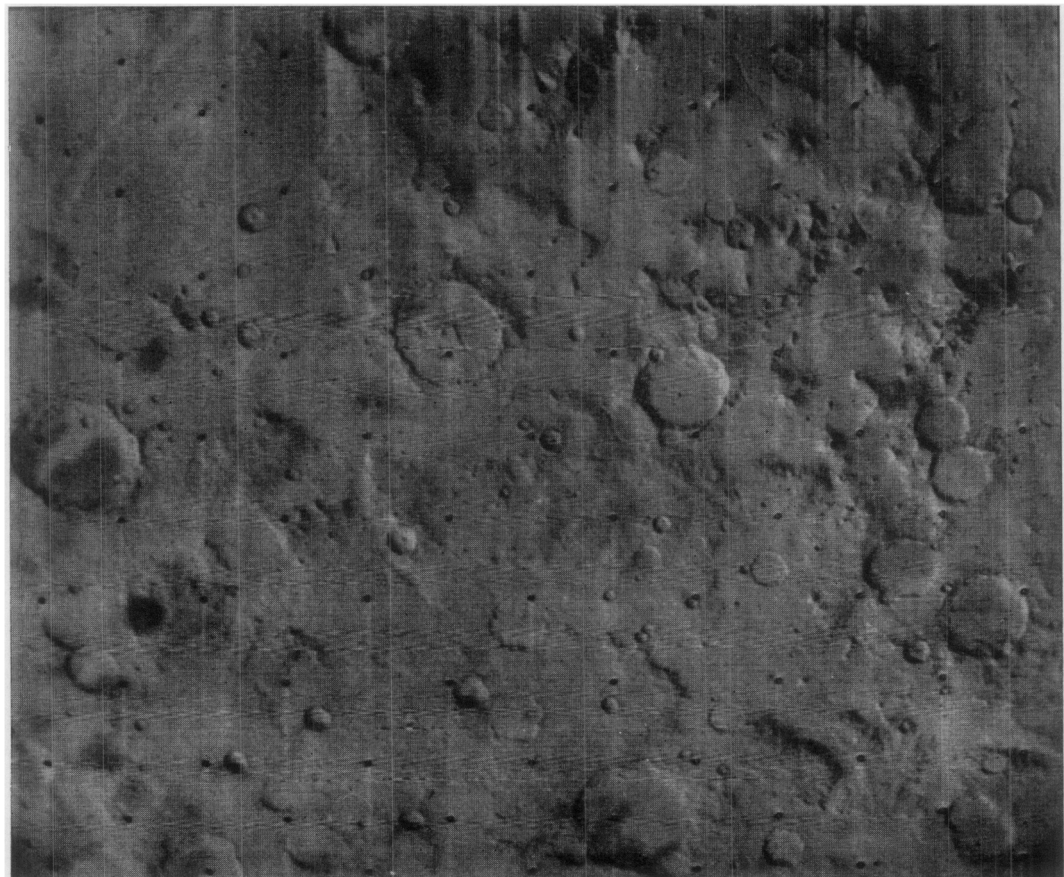


FIG. 18. Type area of mountainous terrain (mt), the large, widely-spaced multipeaked mountains in the upper third of the picture. Cratered plains (cp) and moderately cratered terrain present locally in bottom half of picture. The mountains are vaguely elongate in a direction roughly concentric to the Libya basin, centered northeast of the picture. They probably were formed by uplift and fracturing when the Libya basin formed. A-frame 4188-54, centered at 1.5° S and 279.5° W.

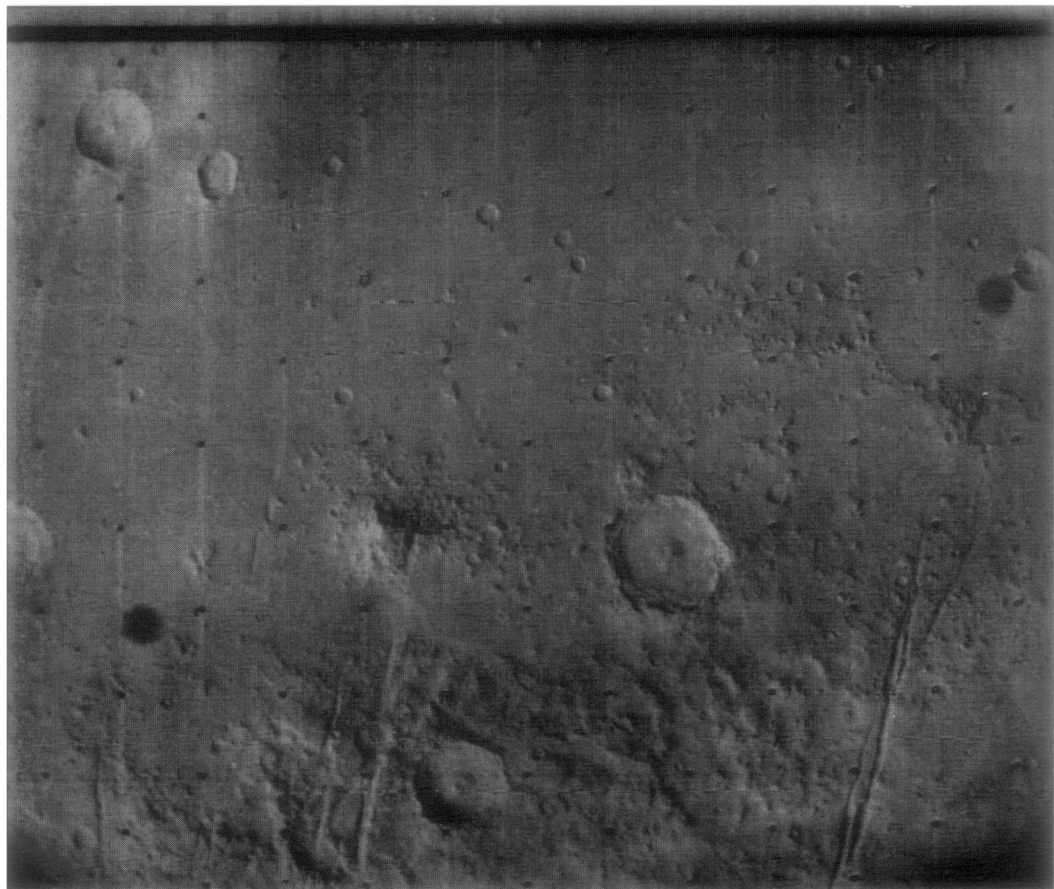


FIG. 19. Type area of knobby terrain (kt), the closely packed, small, sharp-appearing peaks. Some peaks are embayed by plains material and others, in the bottom part of the picture, are superposed on rolling terrain. The conspicuous furrows are probably part of the concentric fracture system of the Libya basin. The knobby terrain may also be related to the basin and be ejecta or fractured prebasin terrain. A-frame 4192-72, centered at 12.5°N and 255.5°W .

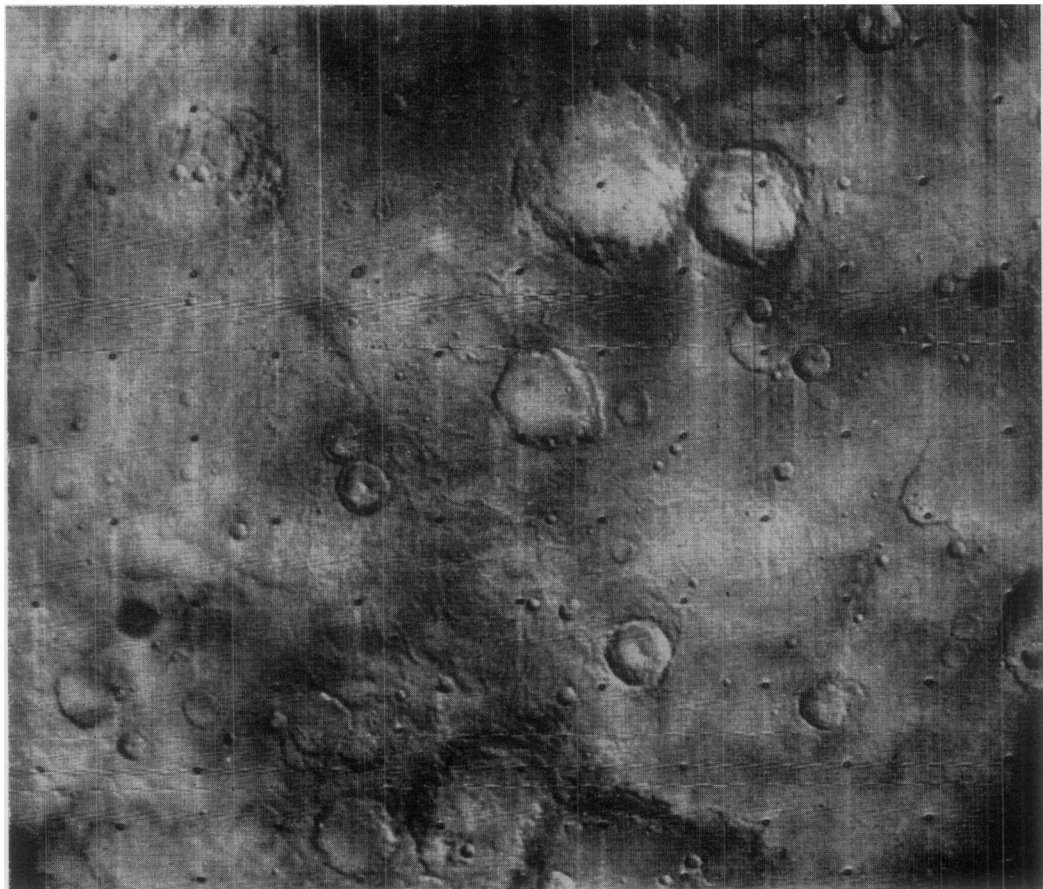


FIG. 20. Sinuous furrows typical of those superposed on the geologic map units in much of the central belt of the mapped area. The furrows are densely packed in the lower central part of the picture and sparser elsewhere; B-frames are needed to see them in some parts of the furrowed terrain. A-frame 4178-69, centered at 9°N and 311°W.

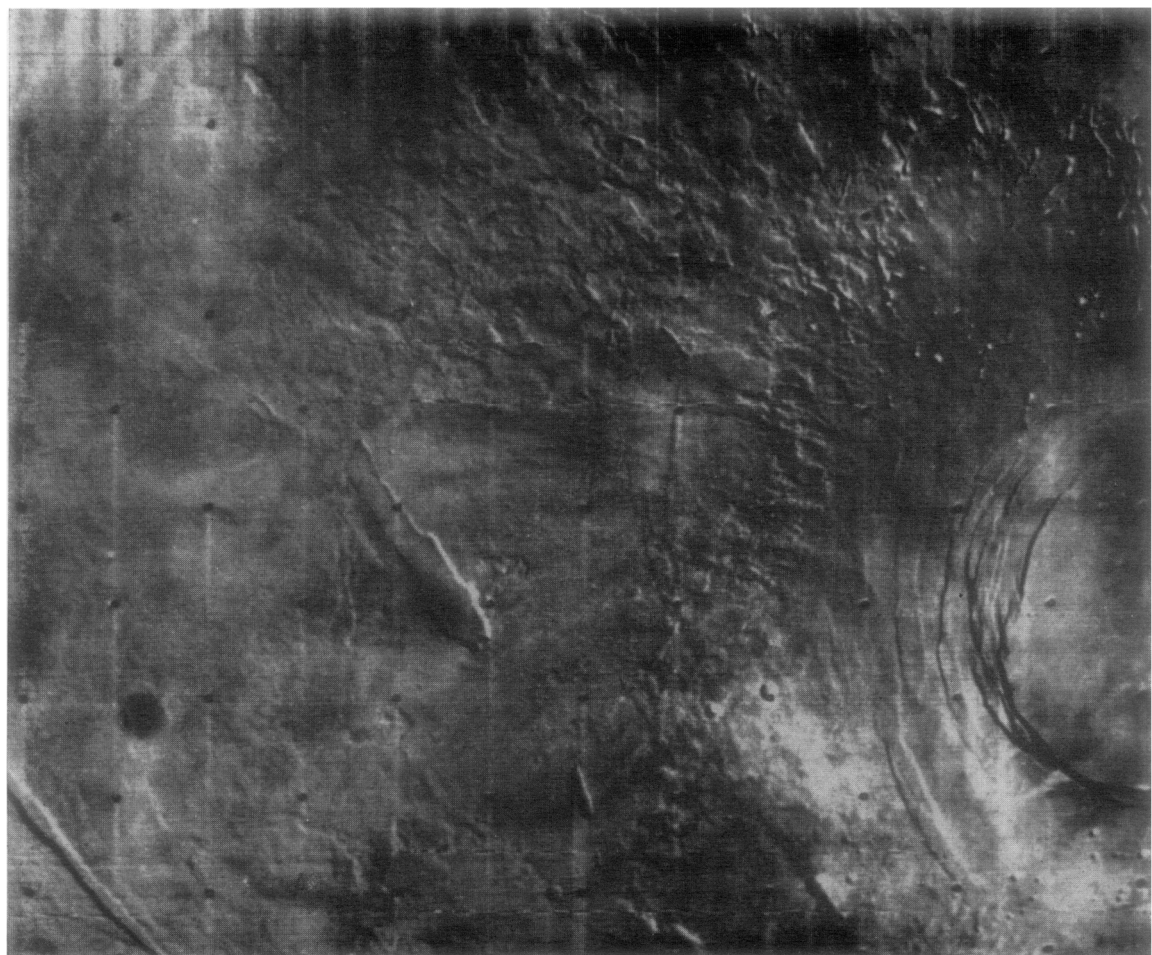


FIG. 21. The west flank of South Spot. Note smooth area marked by circumferential graben surrounding the smooth-floored summit caldera at right of picture. Stubby lobate flows seem to originate from this smooth zone. Numerous small wormy depressions occur within the flank flows. Part of very large ring fracture seen at lower left of picture. A-frame picture.

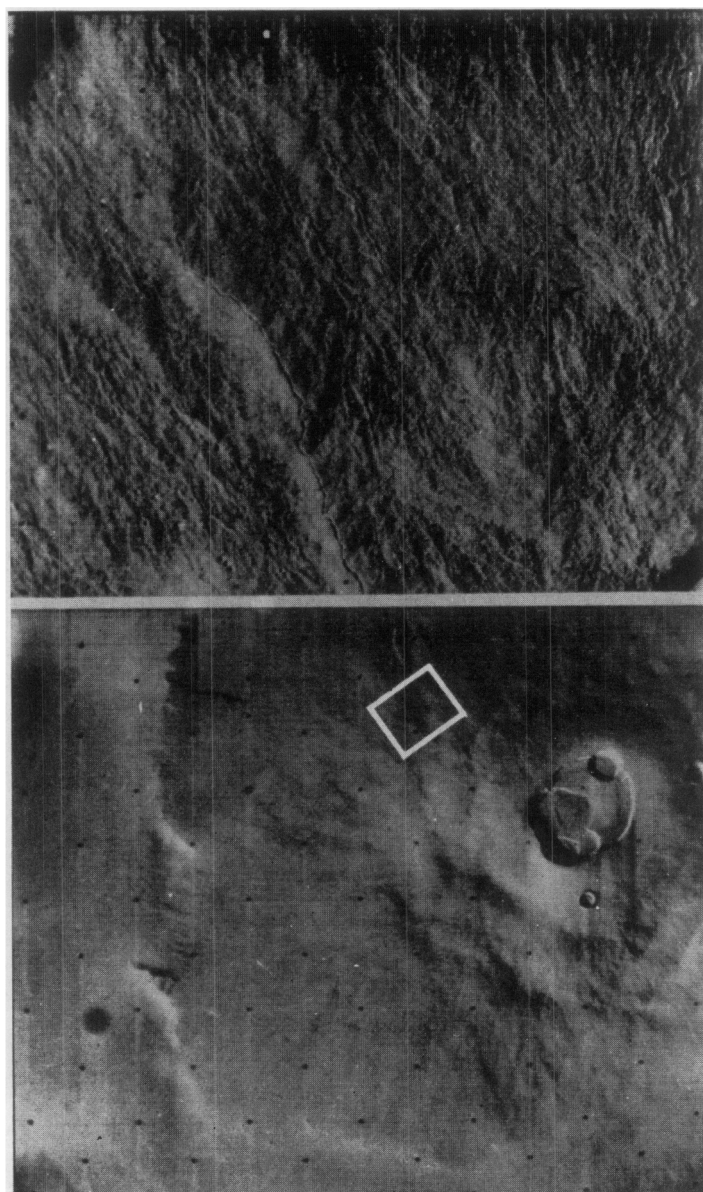


FIG. 22. Composite of A- and B-frame pictures of Nix Olympica. The inset B-frame shows numerous small flow lobes that radiate away from the summit crater. A medial fracture lies along the crest of a gentle radial ridge at left center of picture. This has been interpreted as a possible collapsed lava tube.

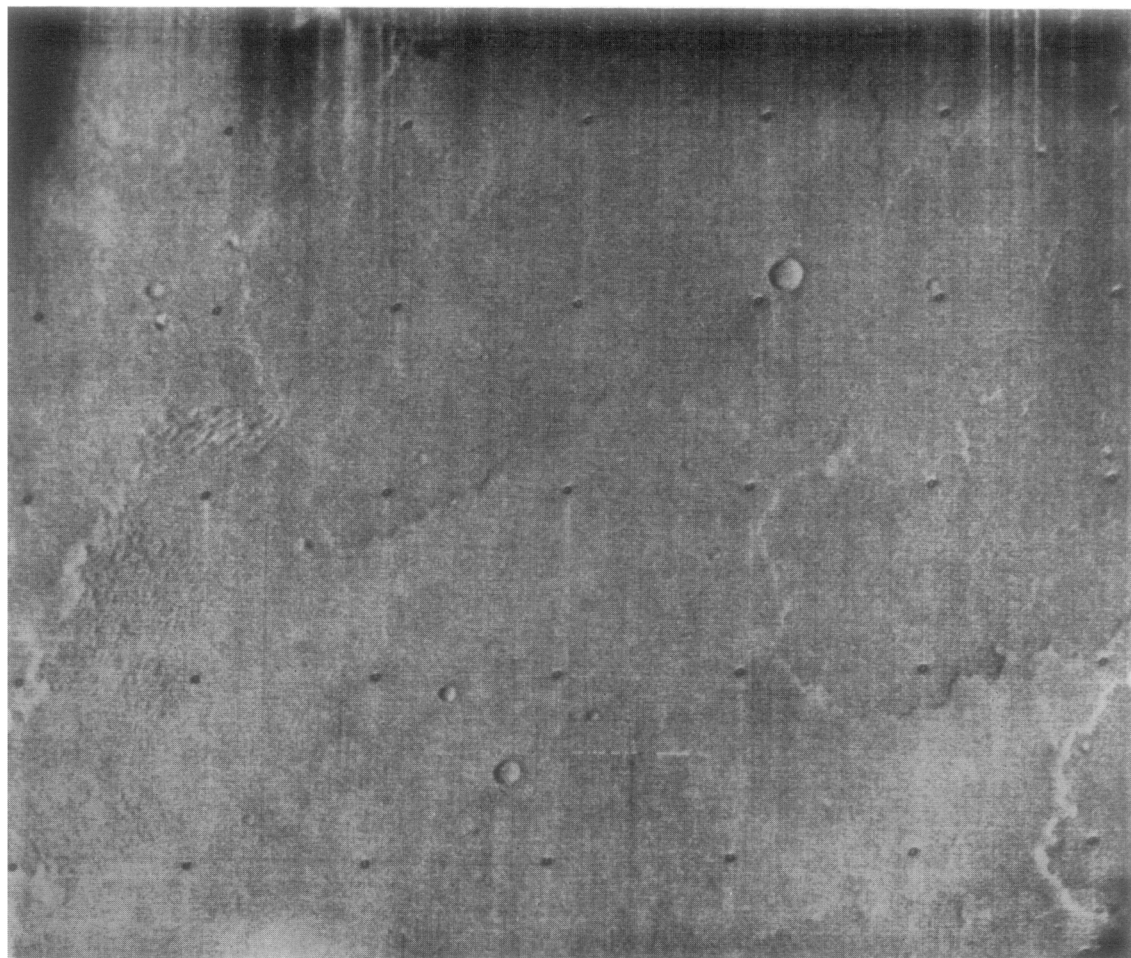


FIG. 23. Flow fronts in the Nix Olympica region within an area mapped as the smooth plains unit. These are common throughout this region and suggest that much of the smooth plains consist of a series of superposed volcanic flows. B-camera frame dimensions across top of picture are approximately 40 km.

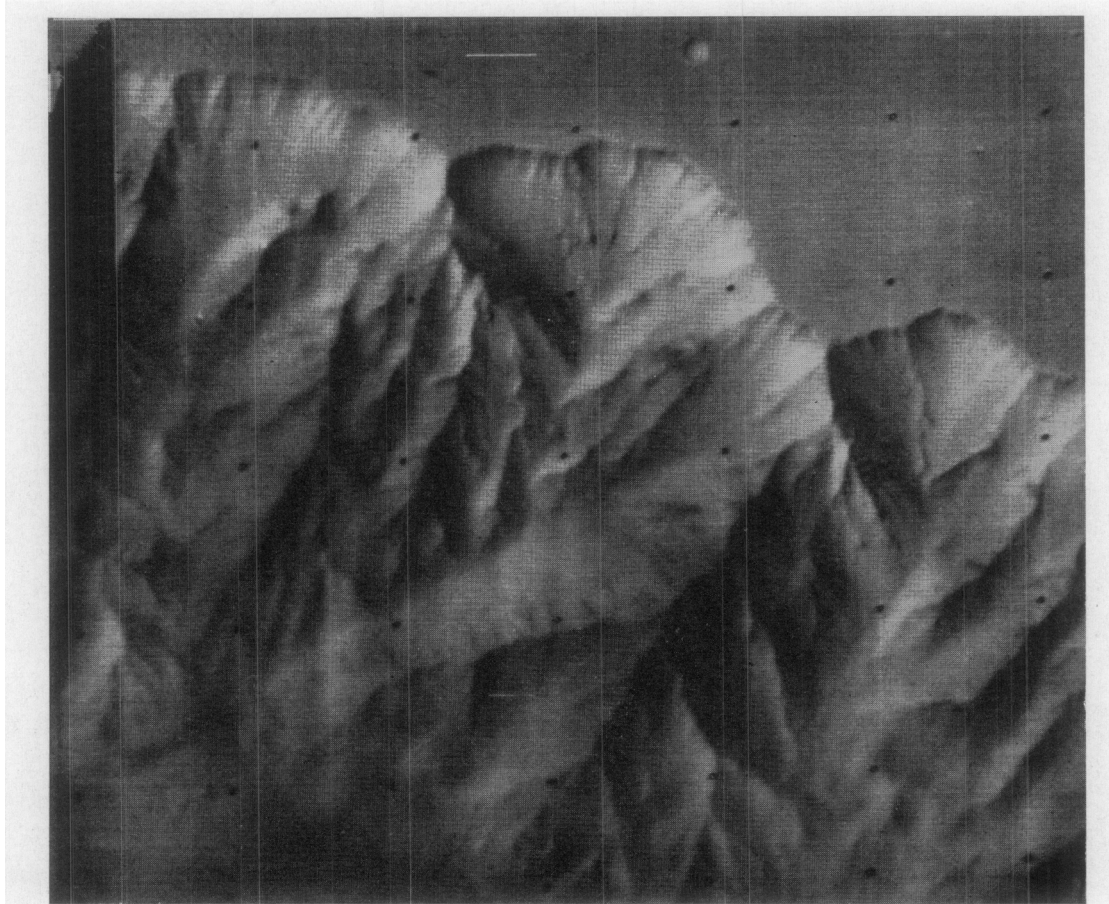


FIG. 24. Ravines and branching sharp narrow divides beneath alcoves on the north wall of the Coprates canyon. A resistant ledge can be seen at the top of the canyon wall along with grooving or fluting of the steep upper parts of the walls. B-camera frame.

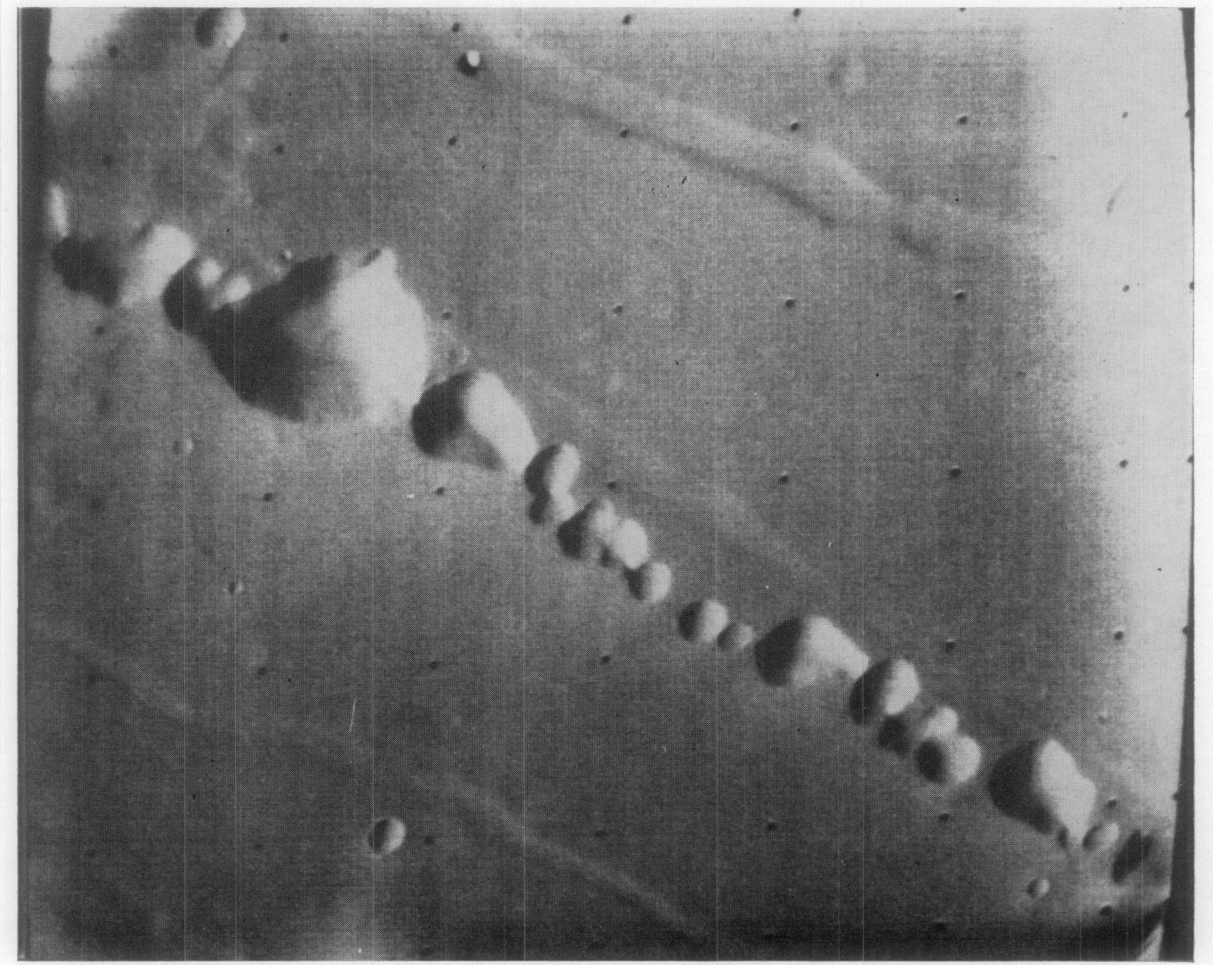


FIG. 25. Chain craters parallel to Coprates canyon system. These features could be volcanic maars or the product of simple collapse and drainage of loose materials into the subsurface. Note graben that parallel the chain craters. B-camera frame.

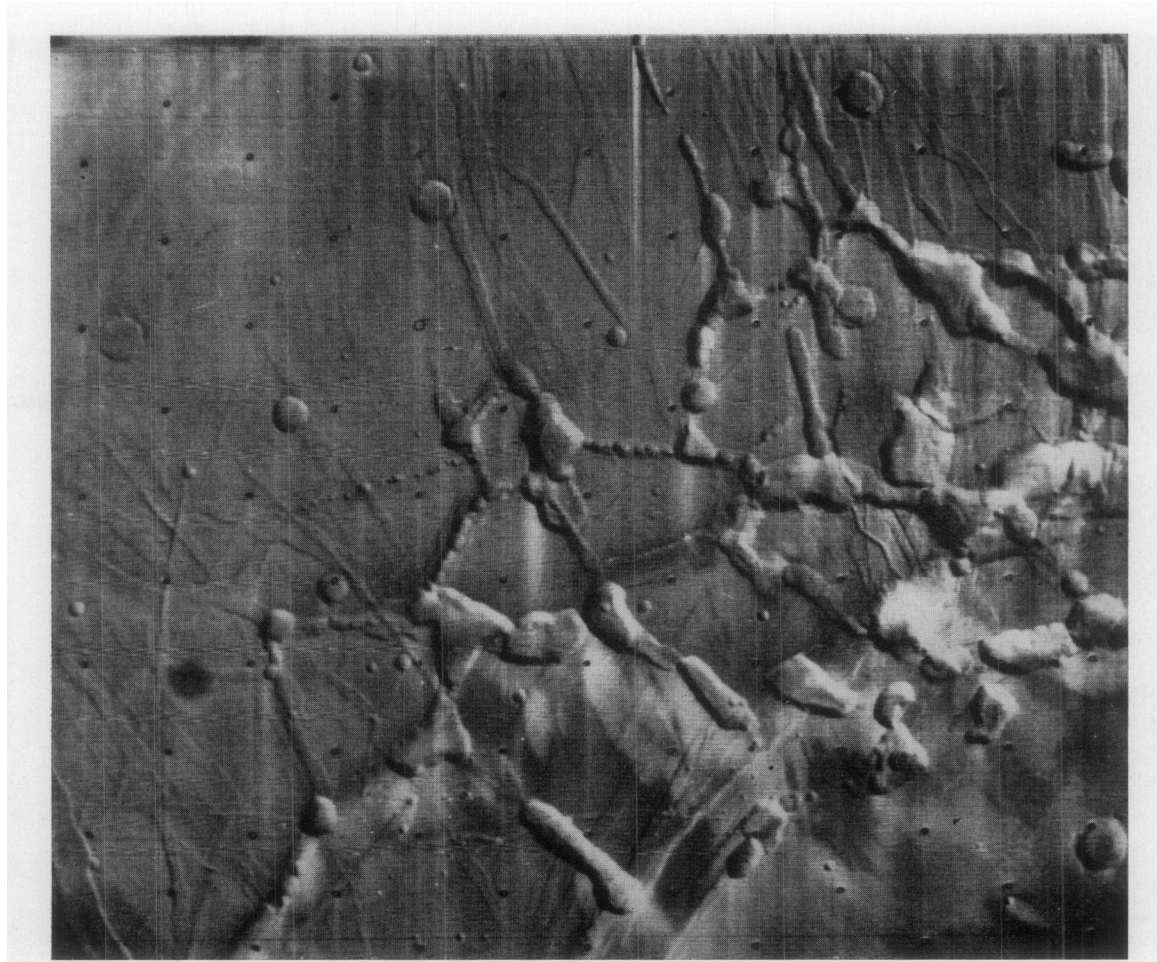


FIG. 26. Westernmost end of Coprates canyon system (the Labyrinth). Note smooth-walled gaping depressions which partially surround flat-topped mesas and small chain craters aligned along some of the fracture zones. The walls of this complex network of depressions are less eroded than are the walls of the canyons to the east suggesting that this area is more youthful than the other parts of the system. A-camera frame.

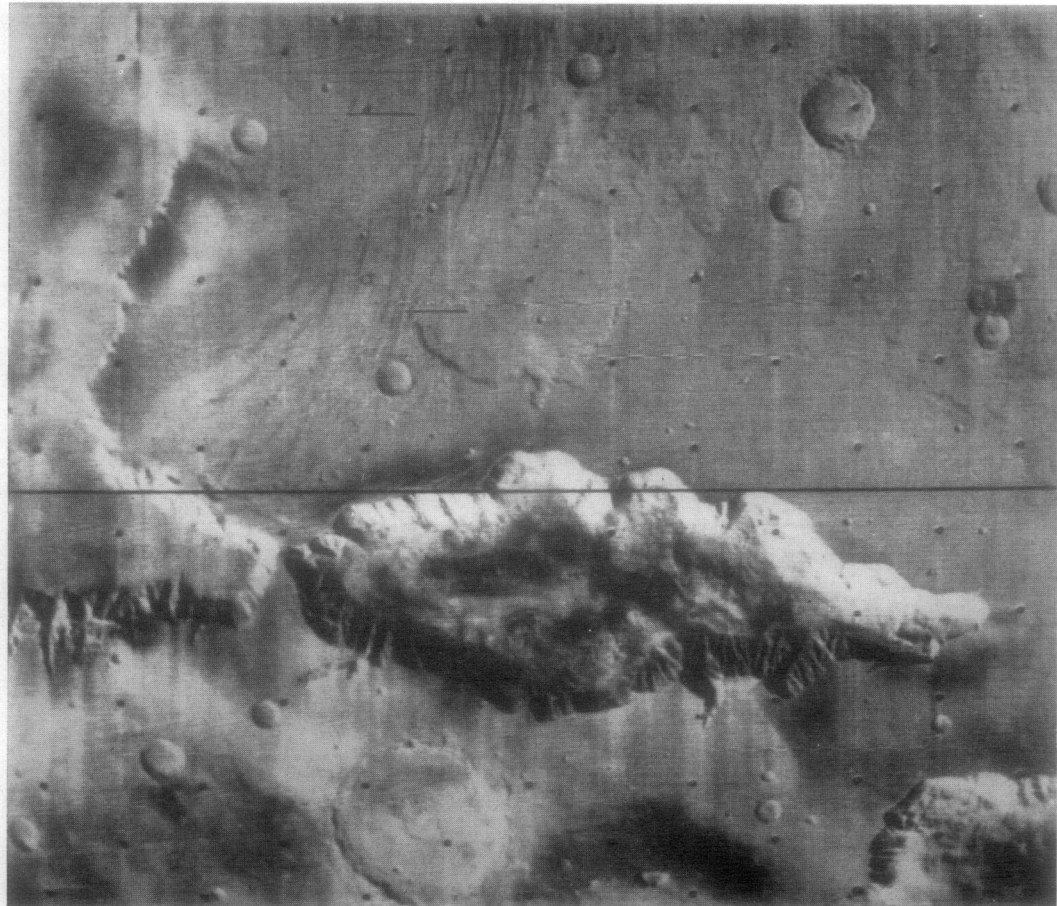


FIG. 27. Completely enclosed canyon some 300 km in length north of the main part of the Coprates canyon system. Note the ravines and gullies on the south wall and the hummocky landslide debris at the base of the smoother north walls which consist of a series of cuspatc alcoves. A-camera frame.

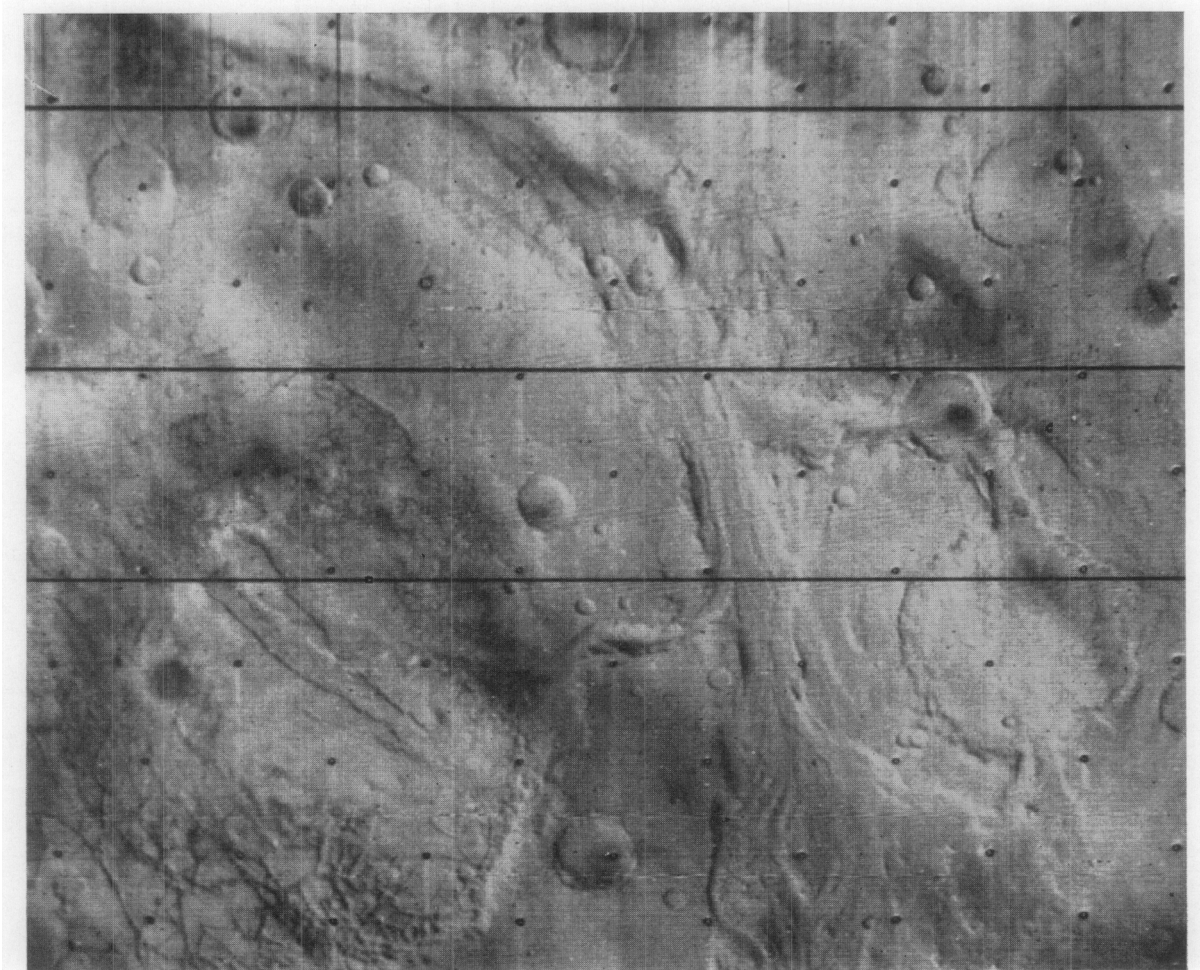


FIG. 28. Braided channel in the southern part of the Oxia Palus region. This is the northern extension of the same channel that is seen in Fig. 14 and it is over 1500 km in length. Note what appear to be channel bars in the lower right center of picture. Chaotic terrain in lower left. A-camera frame.



FIG. 29. Preliminary Mariner 9 crater size-frequency data.

Ground ice may be widespread or perhaps even ubiquitous, in the subsurface of Mars. Local centers of higher-than-normal geo-thermal gradient may have developed and caused subsurface melting that produced liquification of large volumes of loosely consolidated materials. The liquified material may have been contained by a relatively impervious caprock until the reservoir eventually burst, producing a short-lived mudflow of enormous volume. Escape of material to the surface removed support

from the overlying caprock causing extensive caving now exemplified by in the chaotic terrain. Quantitative studies will be necessary to test this preliminary model fully.

The innumerable fine channels of the furrowed terrain present a different problem. Some of these are dendritic and some occur in settings where a subsurface source seems unlikely, for example on the slopes of isolated central peaks within craters. If these are indeed water-erosion

channels, an atmospheric source seems more attractive than a lithospheric one. It is premature to decide the question on either theoretical or observational grounds of whether it might have rained sufficiently at some time in the history of Mars to have produced these small channels.

SURFACE MARKINGS AND EOLIAN ACTIVITY

As indicated from earth-based observations, Mars does not have homogeneous tones and colours. Apart from the polar caps, clouds and dust storms, many tonal differences or so-called albedo markings are observed that must relate to regional variations of topography, composition, or texture of the materials on the surface.

Mariner 6 observations provided new insights into the problem of Mars surface markings (Cutts *et al.*, 1970). Light albedo markings were found to occur frequently upon and around the northern rims of craters on the large dark feature Meridiani Sinus, and dark crescent-shaped features were found on the south part of crater floors. Collectively, the Mariner 6 and 7 observations suggested that the light/dark complexion of Martian features is quite superficial and developed after the formation and erosion of the underlying terrain. It seems likely that the actual distribution of light and dark areas is governed largely by wind transportation, as had been proposed by Sagan and Pollack (1969).

Dominating many Mariner 9 photographs are conspicuous streaks or plumes which originate at a crater, ridge, or scarp and extend up to hundreds of kilometers across the surface of the planet [Sagan *et al.*, 1972 (their Fig. 27)]. At the resolution of the Mariner B-camera, these have no topographic relief. Light and dark plumes are found, and although both exhibit large variations in morphology, they have characteristic differences [Sagan *et al.*, 1972 (their Figs. 12–14)]. Most dark plumes develop from within the floor of a crater and extend outside it; most light plumes develop tangentially to crater rims. Dark plumes in most places contrast sharply with their surroundings; light plumes are usually

of low contrast and have diffuse edges. Where dark plumes are associated with albedo markings on the rim or floor of a crater, dark markings tend to be confined to the floor on the side from which the plume extends. Light markings develop on and around the opposite rim. Light and dark plumes appearing together in a Mariner 9 frame are generally oriented in different directions. In at least one area, Solis Lacus, light and dark plumes intersect. Observations between December and April of 1972 showed the dark plumes to change both shape and direction; no changes in light plumes were observed in this period (Sagan *et al.*, 1972).

The crater plumes do not occur in a random pattern. Large numbers of plumes with similar morphology and similar orientations tend to occur in groups. Some groups are very large, such as the bright plumes in the Hesperia and Memnonia regions. Both of these groups extend for thousands of kilometers and maintain the same orientation. In other areas, such as in the Syrtis Major, the directions change over smaller distances. Dark plumes in the equatorial region extend to the north or southwest. The light plumes extend to the south or southeast. Plumes are few in the polar region below 65°S, but dark markings are found in the northwesterly parts of craters and in the pits and basins that characterize the pitted plains in this part of Mars.

The morphology and distribution of the plumes reinforce earlier ideas that wind moves surficial materials on Mars. We can at present only speculate on the details of the formative mechanism, but most of them must result from deposition, and scouring and sorting of surface materials in the lee of topographic obstructions to the prevailing wind. One series of Mariner 9 photographs (Leovy *et al.*, 1972) shows that a dark area apparently formed behind a bright dust cloud. Dark plumes with high contrasts and sharp boundaries may be the scoured areas that are depleted of the fine particles. The surface now exposed may consist of coarser sand, gravel, or even outcrops of bedrock any one of which account for the lower albedo.

Although the effects of wind on surficial materials appear to be the dominant cause of albedo differences, there are some examples of albedo differences that may reflect differences in exposed bedrock such as those of the cratered plains (cp). The exposed strata in the polar regions of Mars (Murray *et al.*, 1972), and the margins of the shields in the volcanic regions of Mars (Fig. 10) may be additional examples.

Topographic forms, as opposed to albedo markings, probably produced by eolian deposition have been recognized in only a few places. The most spectacular example is the field of transverse dune ridges covering more than 2000 km² on the floor of a large crater at 48°S latitude and 330° longitude [Sagan *et al.*, 1972 (their Fig. 11)]. Spacing between the crests of individual dune ridges is 1–2 km, becoming smaller near the edges of the field, as in terrestrial dune fields. Other dune fields are found in the south polar area. Wind erosion has probably affected much of the surface. In the south polar region especially, smoothly curved slopes, streamlined hills and hollows, and long parallel V-shaped grooves reminiscent of terrestrial yardangs are indicative of wind scouring. Deflation, perhaps in combination with ablation of frozen volatiles, may have played a major role in shaping the surface, particularly in the pitted terrain (Murray *et al.*, 1972). Outside the polar region, probable wind-eroded forms are less striking. However, everywhere on Mars, ridges typically have concave slopes meeting at a sharp crest suggestive of sculpturing by the wind. The general softness of crater rims in contrast with those on the Moon further suggests eolian activity. The lineaments of the grooved terrain (gt) and less extensive patches of similar appearance elsewhere may be fractures etched out by wind scouring.

GEOLOGIC HISTORY

A very generalized geologic history of Mars can be determined from the relations between the units portrayed on the sketch maps of Figs. 1–4. The map explanation,

Fig. 5, shows the inferred order of formation of this deliberately limited number of units. Uncertainties or observable ranges in relative age assignment are indicated by brackets. Units arranged horizontally are considered to be essentially contemporaneous. Later, more detailed mapping will certainly lead to a more refined and rigorous stratigraphy.

Many overlap relations between younger and older units and transections of older units by younger structures can be observed. For example the smooth plains (sp) embay and appear to overlie other units with which they are in contact; the chaotic terrain clearly has formed at the expense of adjacent units. In addition, crater frequency distributions differ markedly between most of the units mapped. Crater density and the morphologic freshness of scarps, ridges, and other landforms are additional relative age criteria, although because of the more dynamic nature of Mars, both are less rigorous in application than on the Moon. The known presence of numerous large volcanic craters on Mars suggests that crater density may be in part related to local volcanic activity, and morphologic freshness may be partly a function of climatic regime (wind, running fluids, and the effects of permafrost). An additional problem is the lack of extensive basin-related marker horizons such as the Fra Mauro and Hevelius Formations (Wilhelms, 1970) which helped to establish a time-stratigraphy for the Moon. Nevertheless, superposition and transection relations, crater density, and morphologic freshness should give first-order approximations of relative age if the majority of the craters are of impact origin and the climatic variations within the equatorial region not too severe.

Accordingly, the oldest unit mapped is almost certainly the densely cratered terrain (dc), which is saturated with craters in the 50–100 km size range. Individually mapped craters and basin-related units (c_i, ci, lt, mt, kt) may be partly contemporaneous with unit dc. As on the Moon, these kinds of units probably represent the most ancient—though not primordial—features still exposed at the

surface. Most of the craters and basins probably record an early epoch of intensive bombardment. Next youngest are the moderately cratered terrain (mc) and the remainder of the individual crater and basin related units such as c., mt, and kt. The relatively smaller size and wider spacing between craters in moderately cratered terrain probably reflect an early episode of crater burial by the deposits that now lie in the intercrater areas.

Although the mountainous terrain (mt) in most places represents relicts of formerly more continuous rims of very large basins, some of the knobby terrain (kt) and lineated terrain (lt) may not be related to basins. The knobby hills conceivably may be of volcanic or structural origin. Regardless of origin, however, overlap and transection relations show that these three units are approximately contemporaneous and apparently younger than the densely cratered terrain.

The next youngest unit is the cratered plains (cp), which fills depressions in all previously discussed units and has a markedly lower crater density than unit mc. In texture, albedo, and distribution it resembles somewhat the lunar maria that flood regionally depressed areas and obscure earlier basin and crater deposits.

The age relations among units younger than those moonlike units are not entirely clear because contact relations are often obscured. Crater populations suggest, however, that the three types of volcanic deposits—shields, domes, and craters—are considerably younger than the cratered plains. The fractured plains (fp) and the grooved terrain (gt) both have a lower crater density than the cratered plains, and therefore are probably younger.

The chaotic terrain (ct), which is formed by breakup of all other mapped units, must be very young. Younger than or contemporaneous with the chaotic terrain are the deposits (ch) that fill the channels and canyons. The formation of both the chaotic terrain and the channel deposits probably spans a considerable period of time. Locally, some chaotic terrain appears to give rise to channels, but the

chaotic terrain in the region near 40°W longitude and 10°N latitude appears to be fluvially scoured and older than the channel in which it lies. Younger than all these units are the smooth plains (sp), which flood or partly flood all previously discussed units.

The age relations between the chaotic terrain to the east, the main canyon system, and the so called "labyrinth" to the west and at the head of the canyon are of particular interest. Neither the steep walls of the labyrinth nor the sides of the large slabs and blocks that comprise the chaotic terrain show the degree of ravine development and gullying seen on the canyon walls, although they locally approach them in height. This suggests that the features at both the east and west ends of the canyon are younger in age.

One of the most striking characteristics of Martian volcanism is its marked regional distribution pattern. Almost all of the volcanic shields, domes and craters lie between 50–250°W and N of latitude 20°S. The volcanic plains that constitute part of unit sp appear to have a wider distribution, but just how wide is not known because of the difficulty of detecting the subtle flow features without more extensive B-camera coverage than now available. Other probable volcanic features such as domes and craters have been identified outside the region mapped. They tend, however, to be scattered and not coincident with regional topographic highs as are the large shields of the Tharsis region.

The intriguing question of the relative ages of the major volcanic structures and the canyons cannot be unequivocally answered at this time on the basis of direct photogeologic evidence. A suggestion is contained, however, in their relations to the units with which they are in contact. The smooth plains (sp) appears to embay the large shields such as Nix Olympica; the canyons, channels, and chaotic terrain (ch and ct) appear locally to cut into or to have developed at the expense of parts of the smooth plains. If the smooth plains are everywhere the same age, which is unlikely, the volcanic shields would be

older than the canyons, channels, and chaotic terrain.

The prospects of utilizing quantitative crater studies to gain additional information about the evolution of Mars are good because its surface is clearly divisible into units of widely differing crater density. For example, the Sabaeus Sinus and Syrtis Major regions are heavily cratered, whereas the region around the Nix Olympica shield volcano complex is very sparsely cratered. It is generally recognized from lunar studies that crater frequency data are useful for relative age assessments and as terrain descriptors but that the method has severe limitations when it comes to absolute age determinations.

Fig. 29 shows some preliminary crater size-frequency data. The data points are averages of counts for several photographs in each of the regions listed. The cratered provinces refer to the Sinus Sabaeus, Deucalionis Regio, and Mare Sirenum regions which are among the most heavily cratered parts of Mars. The uncratered provinces refer to the Solis Lacus, Nix Olympica, and Elysium regions which are among the least cratered regions. The counts on Nix Olympica refer to the shield volcano only; this very restricted area is the least cratered region of its size so far counted, although the floor of Hellas and similar smooth plains areas could be even less cratered.

The cratered province has a considerably greater crater density than the lunar maria. Earlier published studies of Mariner 6 and 7 data suggest that these regions are billions of years old and retain craters dating to a time when the cratering rate was greater than it is now. Therefore simple linear scaling to the age of the lunar maria cannot give a meaningful age for these regions. The pronounced break in slope near $D = 64\text{ km}$, and the region of gentle slope from $D = 6\text{--}64\text{ km}$, may be one indication of past erosion cycles.

Nix Olympica is sparsely cratered so that scaling to the age of the lunar maria, assuming a constant cratering rate in recent geological time, is meaningful if the craters detected on its slopes are of impact origin (the summit calderas are

ignored). The crater retention age of the surface is given by:

$$T = 3.5 \times \frac{N\delta}{N\zeta} \times \frac{F\zeta}{F\delta} \times f \text{ (aeons)}$$

where 3.5 aeons is the assumed mean age of the lunar maria, N is the crater density, F is the cratering rate, and f is a correction factor for the difference in impact velocity of bodies striking the two surfaces. From Fig. 29, Nix Olympica has about 1/14 the crater density of the average lunar mare. Various sources, such as Mariner 4 data and calculations of asteroid cratering of Mars, indicate that the cratering rate on Mars is about 10 times that on the Moon, with an uncertainty of a factor 2 or 3. The factor f is about 1.6 (Hartmann, 1966). These data give a crater retention age for Nix Olympica of about 4×10^7 years, with an uncertainty of at least a factor 2 or 3.

MAJOR CONCLUSIONS

Mariner 9 has shown that Mars is geologically far more heterogeneous than previously suspected from the earlier flyby missions. The analyses to date indicate convincingly that it has a geological style of its own different from that of either the Earth or Moon, and suggest that it represents a body intermediate in its evolutionary sequence somewhere between the Earth and Moon. It is now tempting to consider Mars as a planet that has partly made the transition from a relatively primitive impact-dominated (but not primordial) body like the Moon to an orogenically mobile, volcanically active, water-dominated planet like the Earth. Phobos and Deimos (Pollack *et al.*, 1972) are clearly the most primitive solar system bodies closely investigated to date.

Like the Moon, Mars shows extensively cratered regions as well as numerous large circular basins. The basins, some of which are larger than any lunar basin, seem to exercise less control on the regional topography and distribution of the volcanic units than they do on the Moon.

The crater and basin terrains and the plains material that fills depressions in it are reminiscent of the Moon. But over much of the planet, the later parts of the Martian geological record are punctuated by huge and spectacular tectonic and volcanic features, not moonlike and only partly earthlike, that have destroyed or covered its earlier crater and basin aspect.

Extensive tectonic activity has occurred in huge regions of Mars. Much of this can be ascribed to circumferential tension in the upper parts of the lithosphere and to local doming. No shear or compressional features have been identified to date.

Volcanism has also played an important role in shaping the surface of Mars and probably has contributed in great part to its tenuous atmosphere. Martian volcanism is dramatically more varied and may span a larger part of the planet's history than lunar volcanic activity. Preliminary crater frequency studies point to the possibility that the major shield volcanos, calderas, plains, and other volcanic features could be relatively young.

Erosion and sedimentation, neither of them related to impact cratering, has occurred on a planetwide scale and surface modification processes are more widespread than previously envisioned. Erosion channels and depositional features abound, commonly related geographically and probably genetically to terrain that has collapsed chaotically. Extensive transport of materials has occurred in these channels, and moving fluids probably in episodic surges seem to be the only possible mechanism by which this can be explained, that is consistent with the present observational data.

Mars has clearly undergone a different proportionate mix of major surface-shaping processes than the Earth; the interplay between impact, volcanism, tectonism, and various erosion and sedimentation processes is clearly distinctive. Elucidation of these relations certainly will be the major fruit of the Mariner 1971 mission and should contribute significantly to a better understanding of the Earth.

Most markings observed by Mariner 9 seem to be surficial and of probable

eolian origin. They are partly controlled by topographic features such as craters and scarps and appear to be excellent indicators of both past and recent wind regimes.

ACKNOWLEDGMENTS

G. W. Colton and Joseph Ververka reviewed the manuscript and made numerous helpful suggestions. Colton also helped review and expedite production of the geologic maps. Joseph Boyce also helped in the original compilation of the maps. Special thanks are extended to James Van Divier, Carl Zeller, Roger Carroll, and William Miller for their efficient and timely help in photo reproduction and the drafting of the various illustrations. The original base materials were prepared under the direction of R. M. Batson. The work contained in this report was done under the auspices of the Mars Mariner 1971 Project, Jet Propulsion Laboratory, California Institute of Technology mostly under contract WO-8122.

REFERENCES

- CUTTS, J. A., SODERBLOM, L. A., SHARP, R. P., SMITH, B. A., AND MURRAY, B. C. (1971). The surface of Mars: 3. Light and dark markings. *J. Geophys. Res.* **76**, 343.
- HARTMANN, W. K. (1966). Martian cratering. *Icarus* **5**, 565.
- LEIGHTON, R. B., AND MURRAY, B. C. (1966). Behavior of carbon dioxide and other volatiles on Mars. *Science* **153**, 136.
- LEOVY, C., BRIGGS, G. A., YOUNG, A. T., SMITH, B. A., POLLACK, J. B., SHIPLEY, E. N., AND WILDEY, R. L. (1972). The Martian atmosphere: Mariner 9 television experiment progress report. *Icarus* **17**, 373.
- MASURSKY, H. et al. (1971). Mariner 9 television reconnaissance of Mars and its satellites: Preliminary results. *Science* **175**, 294.
- MCCAULEY, J. F., AND WILHELM, D. E. (1971). Geological provinces of the near side of the Moon. *Icarus* **15**, 363.
- MURRAY, B. C., SODERBLOM, L. A., SHARP, R. P., AND CUTTS, J. A. (1971). The surface of Mars: 1. Cratered terrains. *J. Geophys. Res.* **76**, 313.
- MURRAY, B. C., SODERBLOM, L. A., CUTTS, J. A., SHARP, R., MILTON, D., AND LEIGHTON, R. (1972). Geological framework of the south polar region of Mars. *Icarus* **17**, 328.
- POHN, H. A., AND OFFIELD, T. W. (1970). Lunar crater morphology and relative-age determination of lunar geologic units—pt. 1.

- Classification. In Geological Survey Research 1970: U.S. Geol. Survey Prof. Paper 700-C, C153.
- POLLACK, J., VEVERKA, J., NOLAND, M., SAGAN, C., HARTMANN, W., DUXBURY, T., BORN, G., MILTON, D., AND SMITH, B. (1972). Mariner 9 television observations of Phobos and Deimos. *Icarus* **17**, 394.
- SAGAN, C. (1971). The long winter model of Martian biology. *Icarus* **15**, 511.
- SAGAN, C., AND POLLACK, J. B. (1969). Wind-blown dust on Mars. *Nature, London* **223**, 791.
- SAGAN, C., VEVERKA, J., FOX, P., DUBISCH, R., LEDERBERG, J., LEVINTHAL, E., QUAM, L., TUCKER, R., POLLACK, J., AND SMITH, B. (1972). Variable features on Mars: Preliminary Mariner 9 television results. *Icarus* **17**, 346.
- SHARP, R. P., SODERBLOM, L. A., MURRAY, B. C., AND CUTTS, J. A. (1971). The surface of Mars 2. Uncratered terrains. *J. Geophys. Res.* **76**, 331.
- SIMKIN, T., AND HOWARD, K. A. (1970). Caldera collapse in the Galapagos Islands, 1968. *Science* **169**, 429.
- WILHELM, D. E. (1970). Summary of lunar stratigraphy—Telescopic observations. U.S. Geol. Survey Prof. Paper 599-F, F1.
- WILHELM, D. E., AND McCUALEY, J. F. (1971). Geologic map of the near side of the Moon. U.S. Geol. Misc. Geol. Inv. Map I-703.